J Eng Math (2008) 61:111–132
DOI 10.1007/s10665-007-9188-9

Thermomechanically coupled micromechanical analysis of multiphase composites

Jacob Aboudi

Received: 4 October 2006 / Accepted: 8 August 2007 / Published online: 9 September 2007

Abstract One- and two-way thermomechanically coupled micromechanical analyses of multiphase composites are presented. In the first type of thermomechanical coupling, a constant temperature that affects the mechanical field only is prescribed at any point of the composite's constituents. In the two-way thermomechanical coupling, on the other hand, a mutual interaction exists between the mechanical and temperature fields. It is shown that the macroscopic coupled energy equation that is established from a homogenization procedure cannot provide reliable information about the induced temperature that is caused by an applied far-field mechanical loading of the composite. The details of the induced temperature-field variations can be obtained, on the other hand, by the derived two-way thermomechanically coupled micromechanical analysis, thus enabling the identification of critical hot spots in the mechanically loaded composite. Results exhibit, in particular, the induced temperature field in metal-matrix and polymer-matrix composites.

Keywords High-fidelity generalized method of cells · Homogenization · Micromechanical analysis · Thermomechanical coupling

1 Introduction

There is a considerable amount of research that incorporates the thermomechanical coupling (TMC) between mechanical and thermal effects in micromechanical analyses of composites; see the books by Christensen [1, Chapter 9], Aboudi [2], Parton and Kudryavtsev [3], Kalamkarov and Kolpakov [4], Nemat-Nasser and Hori [5] and the review articles by Aboudi [6] and Arnold et al. [7], for example. However, in most of these investigations the thermomechanical coupling (TMC) is one-way, namely, the thermal effects affect the mechanical field (just like in thermal-stress analyses) but not vise versa. Furthermore, whenever a one-way micromechanical analysis is employed, the temperature deviation from a reference temperature is a constant that is prescribed at every point of the composite's phases. In actual situations, there is a two-way TMC in the sense that a mutual thermomechanical interaction between the mechanical and thermal fields exists at every location of the composite's phases. As a result,

J. Aboudi (✉)
Department of Solid Mechanics, Materials & Systems, Faculty of Engineering, Tel-Aviv University, Ramat-Aviv 69978, Israel
e-mail: aboudi@eng.tau.ac.il

a mechanical loading of a composite gives rise to a spatially dependent temperature field that needs to be determined by a suitable two-way TMC micromechanical analysis.

The purpose of the present paper is to generalized a micromechanical model, referred to as "high-fidelity generalized method of cells" (HFGMC), in order to incorporate two-way TMC capability. The HFGMC with one-way coupling is capable to predict the behavior of multiphase inelastic composites with periodic microstructure by employing the homogenization technique. Its accuracy and reliability was demonstrated by Aboudi et al. [8] and [9], by comparisons with analytical solutions that can be established in certain cases and with finite-element solutions. The method has been employed also for the prediction of the behavior of elastoplastic composites with imperfect bonding between the constituents [10], viscoelastic-viscoplastic composites [11], electro-magneto-thermoelastic composites [12], and composites that are subjected to large deformations; see a recent review by Aboudi [13], which includes also references to its predecessor GMC micromechanical model. It should be noted that the HFGMC with one-way TMC has been implemented into the recently developed micromechanics analysis code `MAC/GMC` by NASA Glenn Research Center, which has many user friendly features and significant flexibility; see [14] for the most recent version of its user guides. The predecessor GMC micromechanical model was employed by Williams and Aboudi [15] to investigate two-way TMC of metal matrix composites.

As a result of the offered generalization of the HFGMC model to incorporate the two-way TMC, macroscopic constitutive equations that govern the thermomechanical behavior of the composite are established. These relations are based on the derivation of the mechanical, thermal and inelastic concentration tensors and scalars. These concentration tensors and scalars are established by the homogenization of the periodic composite, in conjunction with the imposition of the coupled equilibrium and energy equations, and by imposing the continuity of tractions, displacements, heat fluxes and temperatures at the interfaces between the various materials, and by the application of the periodic boundary conditions. The latter conditions ensure that the tractions, displacements heat fluxes and temperatures are identical at the opposite boundaries of a repeating unit cell (RUC) that characterizes the periodic composite. These three types of concentration tensors are interrelated due to the TMC effects. The established macroscopic constitutive equations are given in terms of the effective stiffness tensor and the global thermal and inelastic stress tensors. It is worth mentioning that the effective stiffness tensor of the composite involves the mechanical and thermal concentrations tensors.

The present paper is organized as follows. The homogenization procedure for a one-way TMC, from which the effective stiffness and thermal-stress tensors are established, is reviewed in Sect. 2. This section also includes a brief presentation of HFGMC with a one-way TMC for multiphase composites with inelastic constituents. In Sect. 3, the effective thermal-conductivity tensor and the effective specific heat at constant deformation and constant stress are established, together with the macroscopic energy equation which involves the macroscopic thermomechanical effects. A different homogenization procedure that predicts these effective parameters and macroscopic energy equation was previously presented by Ene [16]. As it is presently shown, this macroscopic energy equation is not capable to provide the temperature variations in the composite's phases that are induced by the TMC effects. On the other hand, these temperature variations can be obtained from a detailed two-way inelastic micromechanical analysis, in conjunction with various types of micromechanically established TMC concentration tensors. Applications that show the effect of TMC are given in Sect. 4 for metal-matrix (which involves inelastic flow) and polymer-matrix composites. In these cases, the average of the induced temperature in the composite and the temperature that is predicted by the macroscopic energy equation are shown together with surface plots that exhibit the detailed variation of the induced temperature due to several types of far-field mechanical loadings.

2 One-way thermomechanically coupled micromechanical analysis

In the framework of HFGMC micromechanics that models the behavior of periodic multiphase composites which is described in this section, the homogenization technique, in which the TMC in thermoelastic constituents is one-way, is described. This is followed by the method of solution of the RUC problem.

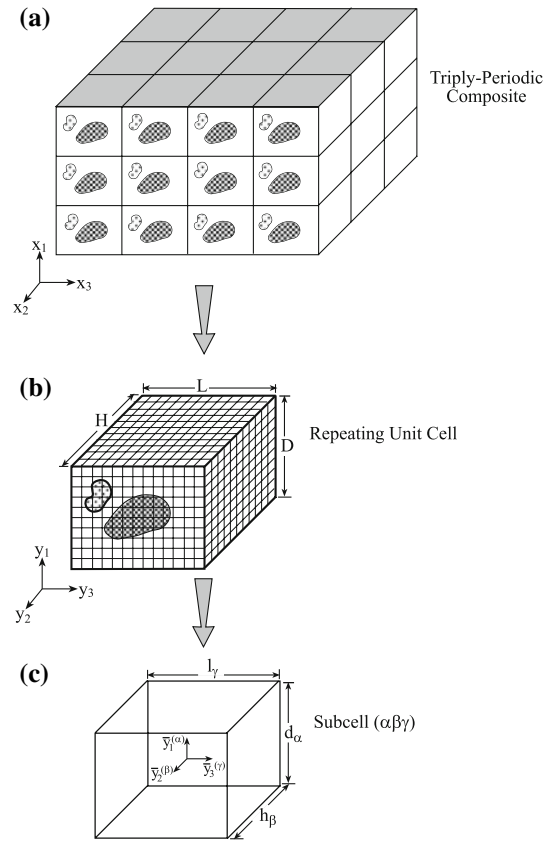

Fig. 1 (**a**) A multiphase composite with triply periodic microstructures defined with respect to global coordinates (x_1, x_2, x_3). (**b**) The repeating unit cell is represented with respect to local coordinates (y_1, y_2, y_3). It is divided into N_α, N_β and N_γ subcells, in the y_1-, y_2- and y_3-directions, respectively. (**c**) A characteristic subcell $(\alpha\beta\gamma)$ with local coordinates $\bar{y}_1^{(\alpha)}$, $\bar{y}_2^{(\beta)}$ and $\bar{y}_3^{(\gamma)}$ whose origin is located at its center

2.1 The homogenization procedure

Consider a multiphase composite in which the microstructures are distributed periodically in the space that is given with respect to the global coordinates (x_1, x_2, x_3); see Fig. 1(a). Figure 1(b) shows the RUC of the periodic composite. In the framework of the homogenization method the displacements are asymptotically expanded as follows

$$\mathbf{u}(\mathbf{x}, \mathbf{y}) = \mathbf{u}^0(\mathbf{x}, \mathbf{y}) + \delta\, \mathbf{u}^1(\mathbf{x}, \mathbf{y}) + \cdots, \tag{1}$$

where $\mathbf{x} = (x_1, x_2, x_3)$ defines the macroscopic (global) coordinate system, and $\mathbf{y} = (y_1, y_2, y_3)$ are the microscopic (local) coordinates that are defined with respect to the RUC. The size of the unit cell is further assumed to be much smaller than the size of the body so that the relation between the global and local systems is

$$\mathbf{y} = \frac{\mathbf{x}}{\delta}, \tag{2}$$

where δ is a small scaling parameter characterizing the size of the unit cell. This implies that a movement of order unity on the local scale corresponds to a very small movement on the global scale.

The homogenization method is applied to composites with periodic microstructures. Thus

$$\mathbf{u}^\xi(\mathbf{x}, \mathbf{y}) = \mathbf{u}^\xi(\mathbf{x}, \mathbf{y} + n_p \mathbf{d}_p) \tag{3}$$

with $\xi = 0, 1, \ldots$, where n_p are arbitrary integer numbers and the constant vectors $\mathbf{d}_p$ determine the period of the microstructure.

Due to the change of coordinates from the global to the local systems, the following relation must be employed in evaluating the derivative of a field quantity:

$$\frac{\partial}{\partial \mathbf{x}} \rightarrow \frac{\partial}{\partial \mathbf{x}} + \frac{1}{\delta}\frac{\partial}{\partial \mathbf{y}}, \quad \text{or} \quad \nabla_{\mathbf{x}} \rightarrow \nabla_{\mathbf{x}} + \frac{1}{\delta}\nabla_{\mathbf{y}}. \tag{4}$$

The quantities $\mathbf{u}^0$ are the displacements in the homogenized region and hence they are not functions of $\mathbf{y}$.

Let

$$\mathbf{u}^0 = \mathbf{u}^0(\mathbf{x}) \equiv \bar{\mathbf{u}} \tag{5}$$

and

$$\mathbf{u}^1 \equiv \tilde{\mathbf{u}}(\mathbf{x}, \mathbf{y}), \tag{6}$$

where the latter are the fluctuating displacements which are unknown periodic functions. These displacements arise due to the heterogeneity of the medium.

The above displacement expansion yields the corresponding strain tensor expansion

$$\boldsymbol{\epsilon} = \boldsymbol{\epsilon}^0_{\mathbf{x}} + \boldsymbol{\epsilon}^1_{\mathbf{y}} + O(\delta), \tag{7}$$

where in conjunction with Eq. (4),

$$\boldsymbol{\epsilon}^0_{\mathbf{x}}(\mathbf{x}) \equiv \bar{\boldsymbol{\epsilon}}(\mathbf{x}) = \frac{1}{2}(\nabla_{\mathbf{x}}\bar{\mathbf{u}} + \bar{\mathbf{u}}\nabla_{\mathbf{x}}) \tag{8}$$

and

$$\boldsymbol{\epsilon}^1_{\mathbf{y}}(\mathbf{x}, \mathbf{y}) \equiv \tilde{\boldsymbol{\epsilon}}(\mathbf{x}, \mathbf{y}) = \frac{1}{2}(\nabla_{\mathbf{y}}\tilde{\mathbf{u}} + \tilde{\mathbf{u}}\nabla_{\mathbf{y}}). \tag{9}$$

This shows that the strain components can be represented as a sum of the average strain $\bar{\boldsymbol{\epsilon}}(\mathbf{x})$ in the composite and a fluctuating strain $\tilde{\boldsymbol{\epsilon}}(\mathbf{x}, \mathbf{y})$. The average of the strain tensor in the RUC is given by

$$\frac{1}{V_y}\int_{V_y} \boldsymbol{\epsilon}\, \mathrm{d}V_y = \frac{1}{V_y}\int_{V_y} (\bar{\boldsymbol{\epsilon}} + \tilde{\boldsymbol{\epsilon}})\, \mathrm{d}V_y = \bar{\boldsymbol{\epsilon}} + \frac{1}{2V_y}\int_{\Gamma_y} [\tilde{\mathbf{u}} \otimes \mathbf{n} + \mathbf{n} \otimes \tilde{\mathbf{u}}]\, \mathrm{d}\Gamma_Y = \bar{\boldsymbol{\epsilon}}, \tag{10}$$

where the divergence theorem has been employed with V_y being the volume of the RUC and Γ_Y is its surface. The resulting surface integral is zero because the fluctuating displacement $\tilde{\mathbf{u}}$ being periodic is equal on opposite sides of the RUC, while the normals $\mathbf{n}$ there have opposite directions. This implies that the average of the fluctuating strain taken over the RUC vanishes. For a homogeneous material it is obvious that the fluctuating displacements and strains vanish identically.

For a composite that is subjected to homogeneous deformation, one can use Eq. (7) to represent the displacement in the form

$$\mathbf{u}(\mathbf{x}, \mathbf{y}) = \bar{\boldsymbol{\epsilon}} \cdot \mathbf{x} + \delta\tilde{\mathbf{u}} + O(\delta^2), \tag{11}$$

where $\bar{\boldsymbol{\epsilon}} \cdot \mathbf{x}$ represents the contribution of the average strain to the total displacement field.

For a thermoelastic anisotropic material the stress tensor $\boldsymbol{\sigma}$ is related to the strain $\boldsymbol{\epsilon}$ tensor and temperature according to the Hooke's law as follows:

$$\boldsymbol{\sigma} = \mathbf{C} : \boldsymbol{\epsilon} - \boldsymbol{\Gamma}\, T, \tag{12}$$

where $\mathbf{C}(\mathbf{x})$ is the fourth-order stiffness tensor of a phase of the composite, $\boldsymbol{\Gamma}(\mathbf{x})$ is its thermal-stress tensor, namely $\boldsymbol{\Gamma} = \mathbf{C} : \boldsymbol{\alpha}$, where $\boldsymbol{\alpha}$ is the coefficient of thermal-expansion tensor, and T is the temperature deviation from a reference temperature. For one-way TMC, the latter is a prescribed constant at every point of the composite's phases. The stiffness and thermal-stress tensors form periodic functions that are defined in the RUC in terms of the local coordinates $\mathbf{y}$ such that

$$\mathbf{C}(\mathbf{x}) = \mathbf{C}(\mathbf{y}), \qquad \boldsymbol{\Gamma}(\mathbf{x}) = \boldsymbol{\Gamma}(\mathbf{y}). \tag{13}$$

Substitution of Eq. (7) in (12) yields

$$\boldsymbol{\sigma} = \mathbf{C} : (\bar{\boldsymbol{\epsilon}}(\mathbf{x}) + \tilde{\boldsymbol{\epsilon}}(\mathbf{x}, \mathbf{y})) - \boldsymbol{\Gamma}\, T + O(\delta). \tag{14}$$

In the absence of a body force, the equilibrium equation yields

$$\left(\nabla_{\mathbf{x}} + \frac{1}{\delta}\nabla_{\mathbf{y}}\right) \cdot \boldsymbol{\sigma} = 0. \tag{15}$$

By equating terms of the order of $1/\delta$ one obtains that

$$\nabla_{\mathbf{y}} \cdot \left[\mathbf{C}(\mathbf{y}) : (\bar{\boldsymbol{\epsilon}}(\mathbf{x}) + \tilde{\boldsymbol{\epsilon}}(\mathbf{x}, \mathbf{y})) - \boldsymbol{\Gamma}(\mathbf{y})\, T\right] = 0. \tag{16}$$

Let us define the following stress quantities

$$\boldsymbol{\sigma}^0 = \mathbf{C}(\mathbf{y}) : \bar{\boldsymbol{\epsilon}}(\mathbf{x}) - \boldsymbol{\Gamma}(\mathbf{y})\, T, \tag{17}$$

$$\boldsymbol{\sigma}^1 = \mathbf{C}(\mathbf{y}) : \tilde{\boldsymbol{\epsilon}}(\mathbf{x}, \mathbf{y}) \tag{18}$$

with the latter being the fluctuating stresses. It follows from Eq. (16) that

$$\nabla_{\mathbf{y}} \cdot \boldsymbol{\sigma}^1 + \nabla_{\mathbf{y}} \cdot \boldsymbol{\sigma}^0 = 0, \tag{19}$$

which is the strong form of the equilibrium equation. It is readily seen that the first term in Eq. (19) involves the unknown fluctuating periodic displacements $\tilde{\mathbf{u}}$, while the second term produces pseudo-body forces whose derivatives are actually zero everywhere except at the interfaces between the phases.

For given values of the average strains $\bar{\boldsymbol{\epsilon}}$ the unknown fluctuating displacements are governed by Eq. (19) subject to periodic boundary conditions that are prescribed at the boundaries of the RUC. In addition to these boundary conditions one needs to impose the continuity of displacements and tractions at the internal interfaces between the phases that fill the RUC. Referring to Fig. 1(b), one observes that the RUC is given by a parallelepiped defined with respect to the local coordinates by $0 \le y_1 \le D$, $0 \le y_2 \le H$, $0 \le y_3 \le L$. Consequently, the periodic boundary conditions are given by

$$\tilde{\mathbf{u}}\,(y_1 = 0) = \tilde{\mathbf{u}}\,(y_1 = D), \quad \overset{(\mathbf{e}_1)}{\mathbf{t}}\,(y_1 = 0) = \overset{(\mathbf{e}_1)}{\mathbf{t}}\,(y_1 = D), \quad \tilde{\mathbf{u}}\,(y_2 = 0) = \tilde{\mathbf{u}}\,(y_2 = H), \tag{20,21,22}$$

$$\overset{(\mathbf{e}_2)}{\mathbf{t}}\,(y_2 = 0) = \overset{(\mathbf{e}_2)}{\mathbf{t}}\,(y_2 = H), \quad \tilde{\mathbf{u}}\,(y_3 = 0) = \tilde{\mathbf{u}}\,(y_3 = L), \quad \overset{(\mathbf{e}_3)}{\mathbf{t}}\,(y_3 = 0) = \overset{(\mathbf{e}_3)}{\mathbf{t}}\,(y_3 = L). \tag{23,24,25}$$

where the tractions on the surfaces of the RUC are denoted by $\overset{(\mathbf{e}_i)}{\mathbf{t}}$, with $\mathbf{e}_i$ being the corresponding unit normal vectors. Any traction vector $\overset{(\mathbf{e}_i)}{\mathbf{t}}$ is expressed in terms of the total stress $\boldsymbol{\sigma}$ which is given by

$$\boldsymbol{\sigma} = \boldsymbol{\sigma}^0 + \boldsymbol{\sigma}^1 + O(\delta), \tag{26}$$

where $\boldsymbol{\sigma}^0$ and $\boldsymbol{\sigma}^1$ are given by Eqs. (17) and (18), respectively. It is also necessary to fix the displacement field at a point in the RUC (e.g. at a corner).

Once a solution of (19), subject to the internal interfacial continuity conditions (displacements and tractions) and periodic boundary conditions (20)–(25) has been established, one can proceed and determine the mechanical and thermal-strain concentration tensors associated with the defined RUC. These tensors express the local strain in the cell in terms of the global applied external strain and temperature (localization). To this end let us define the fourth-order tensor $\tilde{\mathbf{A}}(\mathbf{y})$ and second-order tensor $\mathbf{A}^T(\mathbf{y})$ as follows

$$\tilde{\boldsymbol{\epsilon}}(\mathbf{y}) = \tilde{\mathbf{A}}(\mathbf{y}) : \bar{\boldsymbol{\epsilon}} + \mathbf{A}^T(\mathbf{y})\, T. \tag{27}$$

They relate the fluctuating strain to the applied average strain and temperature. Tensor $\mathbf{A}^T(\mathbf{y})$ is referred to as the thermal-strain concentration tensor. By using Eq. (7), we readily obtain the mechanical strain concentration tensor $\mathbf{A}^M(\mathbf{y})$ as follows

$$\boldsymbol{\epsilon}(\mathbf{x},\mathbf{y}) = \bar{\boldsymbol{\epsilon}}(\mathbf{x}) + \tilde{\mathbf{A}}(\mathbf{y}) : \bar{\boldsymbol{\epsilon}}(\mathbf{x}) + \mathbf{A}^T(\mathbf{y})\, T = [\mathbf{I}_4 + \tilde{\mathbf{A}}(\mathbf{y})] : \bar{\boldsymbol{\epsilon}}(\mathbf{x}) + \mathbf{A}^T(\mathbf{y})\, T \equiv \mathbf{A}^M(\mathbf{y}) : \bar{\boldsymbol{\epsilon}}(\mathbf{x}) + \mathbf{A}^T(\mathbf{y})\, T, \tag{28}$$

where $\mathbf{I}_4$ is the fourth-order identity tensor.

To obtain the strain concentration tensor $\mathbf{A}^M(\mathbf{y})$, a series of isothermal problems must be solved as follows. Solve Eq. (19) in conjunction with the internal interfacial and periodic boundary conditions with $\bar{\epsilon}_{11} = 1$ and all other components being equal to zero. The solution of Eq. (19) readily provides A^M_{ij11} for $i, j = 1, 2, 3$. This procedure is repeated with $\bar{\epsilon}_{22} = 1$ and all other components equal to zero which provides A^M_{ij22}, and so on. Tensor $\mathbf{A}^T(\mathbf{y})$ is computed when $T \neq 0$ in the absence of mechanical effects.

Once the mechanical-strain concentration tensor $\mathbf{A}^M(\mathbf{y})$ has been determined, it is possible to compute the effective stiffness tensor of the multiphase composite as follows. Substitution of $\boldsymbol{\epsilon}$ given by Eq. (28) in (12) yields

$$\boldsymbol{\sigma}(\mathbf{y}) = \mathbf{C}(\mathbf{y}) : \left[\mathbf{A}^M(\mathbf{y}) : \bar{\boldsymbol{\epsilon}} + \mathbf{A}^T(\mathbf{y})\, T\right] - \Gamma(\mathbf{y})\, T. \tag{29}$$

Taking the average of both sides of Eq. (29) over the RUC yields the average stress in the composite in terms of the average strain and temperature via the effective elastic stiffness tensor $\mathbf{C}^*$ and effective thermal-stress tensor $\boldsymbol{\Gamma}^*$, namely

$$\bar{\boldsymbol{\sigma}} = \mathbf{C}^* : \bar{\boldsymbol{\epsilon}} - \boldsymbol{\Gamma}^*\, T, \tag{30}$$

where

$$\mathbf{C}^* = \frac{1}{V_y}\int_{V_y} \mathbf{C}(\mathbf{y}) : \mathbf{A}^M(\mathbf{y})\, \mathrm{d}V_y \tag{31}$$

and

$$\boldsymbol{\Gamma}^* = \frac{1}{V_y}\int_{V_y} \left[\boldsymbol{\Gamma}(\mathbf{y}) - \mathbf{C}(\mathbf{y}) : \mathbf{A}^T(\mathbf{y})\right]\, \mathrm{d}V_y. \tag{32}$$

Alternatively, it is possible to employ Levin's theorem [17] to establish $\boldsymbol{\Gamma}^*$ directly from the mechanical-strain concentration tensor as follows

$$\boldsymbol{\Gamma}^* = \frac{1}{V_y}\int_{V_y} [\mathbf{A}^M]^{\mathrm{tr}}(\mathbf{y}) : \boldsymbol{\Gamma}(\mathbf{y})\, \mathrm{d}V_y, \tag{33}$$

where $[\mathbf{A}^M]^{\mathrm{tr}}$ is the transpose of $\mathbf{A}^M$.

2.2 Solution of the repeating unit-cell problem

The previous analysis has been presented for a multiphase composite with thermoelastic phases in which one-way thermomechanical coupling exists. The HFGMC micromechanical model is employed herein to predict the effective thermo-inelastic behavior of the composite. This theory has been fully described by Aboudi [12] in the case of linearly electro-magneto–thermo-elastic materials. Thus, thermo-elastic phases can be obtained as a special case. The inclusion of an inelastic phase follows the analysis presented by Aboudi el al. [8,9] for the two-dimensional case of continuous fibers. In the present paper, this micromechanical model is briefly outlined in the following.

This model is based on a homogenization technique for composites with periodic microstructure as shown in Fig. 1(a) in terms of the global coordinates (x_1, x_2, x_3). The parallelepiped RUC, Fig. 1(b), defined with respect to local coordinates (y_1, y_2, y_3), of such a composite is divided into N_α, N_β and N_γ subcells in the y_1-, y_2- and y_3-directions, respectively. Each subcell is labeled by the indices $(\alpha\beta\gamma)$ with $\alpha = 1, \ldots, N_\alpha$, $\beta = 1, \ldots, N_\beta$ and $\gamma = 1, \ldots, N_\gamma$, and may contain a distinct homogeneous material. The dimensions of subcell $(\alpha\beta\gamma)$ in the y_1-, y_2- and y_3-directions are denoted by d_α, h_β and l_γ, respectively. A local coordinate system $(\bar{y}_1^{(\alpha)}, \bar{y}_2^{(\beta)}, \bar{y}_3^{(\gamma)})$ is introduced in each subcell whose origin is located at its center; see Fig. 1(c).

The stress $\boldsymbol{\sigma}^{(\alpha\beta\gamma)}$ in subcell $(\alpha\beta\gamma)$ is given, in matrix notation, by

$$\boldsymbol{\sigma}^{(\alpha\beta\gamma)} = \mathbf{C}^{(\alpha\beta\gamma)}\boldsymbol{\epsilon}^{(\alpha\beta\gamma)} - \boldsymbol{\Gamma}^{(\alpha\beta\gamma)}\, T - \boldsymbol{\sigma}^{I(\alpha\beta\gamma)}, \tag{34}$$

where $\mathbf{C}^{(\alpha\beta\gamma)}$ and $\mathbf{\Gamma}^{(\alpha\beta\gamma)}$ are the stiffness and thermal-stress tensors of the material that fills subcell $(\alpha\beta\gamma)$. The inelastic stress $\boldsymbol{\sigma}^{I(\alpha\beta\gamma)}$ is included in order to model multiphase composites with thermo-inelastic phases. The inelastic strain that is related to $\boldsymbol{\sigma}^{I(\alpha\beta\gamma)}$ is governed either by the Prandtl–Reuss equations of classical plasticity or by an appropriate viscoplastic flow rule.

An approximate solution for the displacement field is constructed based on volumetric averaging of the field equations together with the imposition of the periodic boundary conditions and continuity conditions in an average sense between the subcells used to characterize the materials' microstructure. This is accomplished by approximating the fluctuating displacement field in each subcell of the generic cell of Fig. (1c) using a quadratic expansion in terms of local coordinates $(\bar{y}_1^{(\alpha)}, \bar{y}_2^{(\beta)}, \bar{y}_3^{(\gamma)})$ centered at the subcell's midpoint. A higher-order representation of the fluctuating field is necessary in order to capture the local effects created by the field gradients and the microstructure of the composite.

The second-order expansion of the displacement vector $\mathbf{u}^{(\alpha\beta\gamma)}$ in the subcell is given in terms of the local coordinates of the subcell as follows:

$$\begin{aligned}\mathbf{u}^{(\alpha\beta\gamma)} &= \bar{\boldsymbol{\epsilon}}\cdot\mathbf{x} + \mathbf{W}_{(000)}^{(\alpha\beta\gamma)} + \bar{y}_1^{(\alpha)}\mathbf{W}_{(100)}^{(\alpha\beta\gamma)} + \bar{y}_2^{(\beta)}\mathbf{W}_{(010)}^{(\alpha\beta\gamma)} + \bar{y}_3^{(\gamma)}\mathbf{W}_{(001)}^{(\alpha\beta\gamma)} \\ &\quad + \frac{1}{2}\left(3\bar{y}_1^{(\alpha)2} - \frac{d_\alpha^2}{4}\right)\mathbf{W}_{(200)}^{(\alpha\beta\gamma)} + \frac{1}{2}\left(3\bar{y}_2^{(\beta)2} - \frac{h_\beta^2}{4}\right)\mathbf{W}_{(020)}^{(\alpha\beta\gamma)} + \frac{1}{2}\left(3\bar{y}_3^{(\gamma)2} - \frac{l_\gamma^2}{4}\right)\mathbf{W}_{(002)}^{(\alpha\beta\gamma)},\end{aligned} \tag{35}$$

where $\mathbf{W}_{(000)}^{(\alpha\beta\gamma)}$, which is the fluctuating volume-averaged displacement vector, and the higher-order terms $\mathbf{W}_{(lmn)}^{(\alpha\beta\gamma)}$, must be determined from the coupled governing equations (19) as well as the periodic boundary conditions (20)–(25) that the fluctuating field must fulfill, in conjunction with the interfacial continuity conditions between subcells. The total number of unknowns that describe the fluctuating field in the subcell $(\alpha\beta\gamma)$ is 21. Consequently, the governing equations for the interior and boundary cells form a system of $21N_\alpha N_\beta N_\gamma$ algebraic equations in the unknown field coefficients that appear in the quadratic expansions (35).

The final form of this system of equations can be represented symbolically by

$$\mathbf{KU} = \mathbf{f} + \mathbf{g}, \tag{36}$$

where the structural stiffness matrix $\mathbf{K}$ contains information on the geometry and mechanical properties of the materials within the individual subcells $(\alpha\beta\gamma)$ within the cells comprising the multiphase periodic composite. The displacement vector $\mathbf{U}$ contains the unknown displacement coefficients in each subcell that appear on the right-hand side of Eq. (35), namely

$$\mathbf{U} = [\mathbf{U}^{(111)}, \ldots, \mathbf{U}^{(N_\alpha N_\beta N_\gamma)}], \tag{37}$$

where in subcell $(\alpha\beta\gamma)$ these coefficients, which appear on the right-hand side of Eq. (35), are

$$\mathbf{U}^{(\alpha\beta\gamma)} = \left[\mathbf{W}_{(000)}, \mathbf{W}_{(100)}, \mathbf{W}_{(010)}, \mathbf{W}_{(001)}, \mathbf{W}_{(200)}, \mathbf{W}_{(020)}, \mathbf{W}_{(002)}\right]^{(\alpha\beta\gamma)}. \tag{38}$$

The force $\mathbf{f}$ contains information on the thermomechanical properties of the materials filling the subcells, the applied average strains $\bar{\epsilon}_{ij}$ and the imposed temperature deviation T. The inelastic force vector $\mathbf{g}$ appearing on the right-hand side of Eq. (36) contains the inelastic effects given in terms of the integrals of the inelastic strain distributions. These integrals depend implicitly on the elements of the displacement coefficient vector $\mathbf{U}$, requiring an incremental solution procedure of Eq. (36) at each point along the loading path; see [8,9] for more details. It should be noted that, since HFGMC model is based on the implementation of the governing equations (19) and the various interfacial and periodic conditions in the average (integral) sense, there are no derivatives at the boundaries that do not exist and singularities do not arise in Eq. (19).

The solution of Eq. (36) enables the establishment of the following localization relation which expresses the average strain $\bar{\boldsymbol{\epsilon}}^{(\alpha\beta\gamma)}$ in the subcell $(\alpha\beta\gamma)$ in terms of the external applied strain $\bar{\boldsymbol{\epsilon}}$ in the form:

$$\bar{\boldsymbol{\epsilon}}^{(\alpha\beta\gamma)} = \mathbf{A}^{M(\alpha\beta\gamma)}\bar{\boldsymbol{\epsilon}} + \mathbf{A}^{T(\alpha\beta\gamma)} + \mathbf{A}^{I(\alpha\beta\gamma)}, \tag{39}$$

where $\mathbf{A}^{M(\alpha\beta\gamma)}$ is the mechanical-strain concentration matrix of the subcell $(\alpha\beta\gamma)$; $\mathbf{A}^{T(\alpha\beta\gamma)}$ is a vector that involves the current thermoelastic effects in the subcell and $\mathbf{A}^{I(\alpha\beta\gamma)}$ is the corresponding inelastic strain vector. It is worth

mentioning that, whereas $\mathbf{A}^{M(\alpha\beta\gamma)}$ represents a mapping between the global and local strain tensors, $\mathbf{A}^{T(\alpha\beta\gamma)}$ and $\mathbf{A}^{I(\alpha\beta\gamma)}$ do not represent a mapping between the global thermal and inelastic strains in the same sense as $\mathbf{A}^{M(\alpha\beta\gamma)}$. Thus, these two terms may be referred to as thermal and inelastic forcing effects.

The final form of the effective constitutive law of the multiphase thermo-inelastic composite, which relates the average stress $\bar{\boldsymbol{\sigma}}$ and strain $\bar{\boldsymbol{\epsilon}}$, is established by employing the definition of the average stress in the composite:

$$\bar{\boldsymbol{\sigma}} = \frac{1}{DHL}\sum_{\alpha=1}^{N_\alpha}\sum_{\beta=1}^{N_\beta}\sum_{\gamma=1}^{N_\gamma} d_\alpha h_\beta l_\gamma \bar{\boldsymbol{\sigma}}^{(\alpha\beta\gamma)}, \tag{40}$$

where $\bar{\boldsymbol{\sigma}}^{(\alpha\beta\gamma)}$ is the average stress in the subcell.

$$\bar{\boldsymbol{\sigma}} = \mathbf{C}^*\,\bar{\boldsymbol{\epsilon}} - \boldsymbol{\Gamma}^*\,T - \bar{\boldsymbol{\sigma}}^I. \tag{41}$$

In this equation $\mathbf{C}^*$ is the effective elastic stiffness matrix of the composite which is given by the closed-form expression:

$$\mathbf{C}^* = \frac{1}{DHL}\sum_{\alpha=1}^{N_\alpha}\sum_{\beta=1}^{N_\beta}\sum_{\gamma=1}^{N_\gamma} d_\alpha h_\beta l_\gamma\, \mathbf{C}^{(\alpha\beta\gamma)}\,\mathbf{A}^{M(\alpha\beta\gamma)}. \tag{42}$$

In addition, $\boldsymbol{\Gamma}^*$ denotes the effective thermal-stress tensor of the composite. It can be determined from Levin's theorem [17] which directly provides the effective thermal-stress vector $\boldsymbol{\Gamma}^*$ in terms of the individual thermal-stress vectors $\boldsymbol{\Gamma}^{(\alpha\beta\gamma)}$ of the phases and the mechanical-strain concentrations matrices $\mathbf{A}^{M(\alpha\beta\gamma)}$, as follows (see Eq. (33)):

$$\boldsymbol{\Gamma}^* = \frac{1}{DHL}\sum_{\alpha=1}^{N_\alpha}\sum_{\beta=1}^{N_\beta}\sum_{\gamma=1}^{N_\gamma} d_\alpha h_\beta l_\gamma [\mathbf{A}^{M(\alpha\beta\gamma)}]^{\mathrm{tr}}\boldsymbol{\Gamma}^{(\alpha\beta\gamma)}, \tag{43}$$

where $[\mathbf{A}^{M(\alpha\beta\gamma)}]^{\mathrm{tr}}$ denotes the transpose of $\mathbf{A}^{M(\alpha\beta\gamma)}$. The effective coefficients of thermal expansion can be readily obtained from $\boldsymbol{\Gamma}^*$ according to:

$$\boldsymbol{\alpha}^* = \mathbf{C}^{*-1}\boldsymbol{\Gamma}^* \tag{44}$$

Alternatively, it is possible to establish $\boldsymbol{\Gamma}^*$ without utilizing Levin's result. This can be accomplished by employing again Eq. (39), while utilizing the thermal-strain concentration vector $\mathbf{A}^{T(\alpha\beta\gamma)}$, which can be determined by applying a temperature deviation in the absence of mechanical loadings. The final form of the global constitutive relation is given again by Eq. (41), but with $\boldsymbol{\Gamma}^*$ expressed by

$$\boldsymbol{\Gamma}^* = \frac{-1}{DHL}\sum_{\alpha=1}^{N_\alpha}\sum_{\beta=1}^{N_\beta}\sum_{\gamma=1}^{N_\gamma} d_\alpha h_\beta l_\gamma \left[\mathbf{C}^{(\alpha\beta\gamma)}\mathbf{A}^{T(\alpha\beta\gamma)} - \boldsymbol{\Gamma}^{(\alpha\beta\gamma)}\right]. \tag{45}$$

The two expressions (43) and (45) provide identical results.

The global inelastic stress in Eq. (41) is determined from

$$\bar{\boldsymbol{\sigma}}^I = \frac{-1}{DHL}\sum_{\alpha=1}^{N_\alpha}\sum_{\beta=1}^{N_\beta}\sum_{\gamma=1}^{N_\gamma} d_\alpha h_\beta l_\gamma \left[\mathbf{C}^{(\alpha\beta\gamma)}\mathbf{A}^{I(\alpha\beta\gamma)} - \mathbf{R}_{(000)}^{(\alpha\beta\gamma)}\right], \tag{46}$$

where the term $\mathbf{R}_{(000)}^{(\alpha\beta\gamma)}$ represents inelastic stress effects in the phase occupying the subcell $(\alpha\beta\gamma)$.

It is possible to show that the effective stiffness matrix $\mathbf{C}^*$ is symmetric. Following Haj-Ali and Pecknold [18], this can be established by considering the global strain-energy density which, in matrix notation, is given by

$$\frac{1}{2}[\bar{\boldsymbol{\epsilon}}]^{\mathrm{tr}}\bar{\boldsymbol{\sigma}} = \frac{1}{2}[\bar{\boldsymbol{\sigma}}]^{\mathrm{tr}}\bar{\boldsymbol{\epsilon}} \tag{47}$$

Hence

$$\frac{[\bar{\boldsymbol{\epsilon}}]^{\mathrm{tr}}}{DHL}\sum_{\alpha=1}^{N_\alpha}\sum_{\beta=1}^{N_\beta}\sum_{\gamma=1}^{N_\gamma} d_\alpha h_\beta l_\gamma \bar{\boldsymbol{\sigma}}^{(\alpha\beta\gamma)} = \left[\frac{1}{DHL}\sum_{\alpha=1}^{N_\alpha}\sum_{\beta=1}^{N_\beta}\sum_{\gamma=1}^{N_\gamma} d_\alpha h_\beta l_\gamma [\bar{\boldsymbol{\sigma}}^{(\alpha\beta\gamma)}]^{\mathrm{tr}}\right]\bar{\boldsymbol{\epsilon}}. \tag{48}$$

By employing the mechanical portions in Eq. (34) and (39), we may write this expression as

$$[\bar{\boldsymbol{\epsilon}}]^{\mathrm{tr}} \sum_{\alpha=1}^{N_\alpha} \sum_{\beta=1}^{N_\beta} \sum_{\gamma=1}^{N_\gamma} d_\alpha h_\beta l_\gamma \mathbf{C}^{(\alpha\beta\gamma)} \mathbf{A}^{M(\alpha\beta\gamma)} \bar{\boldsymbol{\epsilon}} = \left[\sum_{\alpha=1}^{N_\alpha} \sum_{\beta=1}^{N_\beta} \sum_{\gamma=1}^{N_\gamma} d_\alpha h_\beta l_\gamma [\bar{\boldsymbol{\epsilon}}]^{\mathrm{tr}} [\mathbf{A}^{M(\alpha\beta\gamma)}]^{\mathrm{tr}} [\mathbf{C}^{(\alpha\beta\gamma)}]^{\mathrm{tr}} \right] \bar{\boldsymbol{\epsilon}}. \tag{49}$$

This implies that

$$\sum_{\alpha=1}^{N_\alpha} \sum_{\beta=1}^{N_\beta} \sum_{\gamma=1}^{N_\gamma} d_\alpha h_\beta l_\gamma \mathbf{C}^{(\alpha\beta\gamma)} \mathbf{A}^{M(\alpha\beta\gamma)} = \sum_{\alpha=1}^{N_\alpha} \sum_{\beta=1}^{N_\beta} \sum_{\gamma=1}^{N_\gamma} d_\alpha h_\beta l_\gamma [\mathbf{A}^{M(\alpha\beta\gamma)}]^{\mathrm{tr}} [\mathbf{C}^{(\alpha\beta\gamma)}]^{\mathrm{tr}}. \tag{50}$$

This relation shows that $\mathbf{C}^*$ in Eq. (42) is indeed symmetric: $\mathbf{C}^* = [\mathbf{C}^*]^{\mathrm{tr}}$.

Extensive comparisons between the predicted effective thermo-elastic constants provided by the HFGMC model with finite-element solutions can be found in [19]. Numerous verifications of the reliability of the predicted inelastic behavior of composites under various types of thermo-elastic loadings can be found in [8,9].

We conclude this section by mentioning that while the HFGMC theory seems like the finite-element procedure in that it considers a discretized geometry upon which interfacial and periodic conditions are imposed, the formulation is completely unrelated to the finite-element approach. The HFGMC theory is not based on a variational principle, nor does it employ the concept of nodes. In the present approach, exact displacement-field continuity between adjacent domains is not required, whereas the finite-element procedure requires satisfaction of exact displacement continuity at the nodes. The governing equations in the present theory are enforced in a volume-averaged sense for each subcell, while the continuity of tractions, displacements and periodic conditions are imposed in the integral sense (in the traditional finite-element analysis tractions continuity is not imposed). This feature renders the HFGMC theory far less sensitive to mesh refinement as compared to the finite-element procedure since, even with a coarse "mesh" representation, the theory is unconditionally convergent in the sense that the governing conditions are satisfied. As in the finite-element method, refinement of geometric discretization does lead to improved field accuracy within the HFGMC theory, although the effect is less pronounced.

3 Two-way thermomechanically coupled micromechanical analysis

In this section, the coupled energy equation for anisotropic thermo-elastic materials is presented together with the associated coefficients of heat conductivities and heat capacities. Next, the homogenization technique for multiphase composites in which the thermo-elastic constituents are modeled by a two-way TMC is presented. This is followed by the method of solution of the RUC problem in the framework of HFGMC model.

3.1 The energy equation

Consider a homogeneous thermo-elastic anisotropic material. By expanding the Helmholtz free-energy function into a power series of the second order and employing the first and second laws of thermodynamics, Christensen [1, Chapter 9] obtained the constitutive equation (12) for the stress tensor and the following expression for the entropy s per unit mass

$$\rho s = \boldsymbol{\Gamma} : \boldsymbol{\epsilon} + \rho c_v \frac{T}{T_R}, \tag{51}$$

where ρ is the mass density, c_v is the specific heat at constant deformation:

$$c_v = T_R \left[\frac{\partial s}{\partial T} \right]_{\boldsymbol{\epsilon}} \tag{52}$$

and T_R is a reference temperature. In addition, the energy equation is given in the absence of heat sources by

$$\rho c_v \frac{\partial T}{\partial t} + \nabla \cdot \mathbf{q} = -T_R \, \boldsymbol{\Gamma} : \frac{\partial \boldsymbol{\epsilon}}{\partial t}, \tag{53}$$

where t is the time and $\mathbf{q}$ is the heat flux which is related to the second-order thermal-conductivity tensor $\mathbf{k}$ by the Fourier's law

$$\mathbf{q} = -\mathbf{k} \cdot \nabla T. \tag{54}$$

Alternatively, the Gibbs free energy rather than the Helmholtz energy function can be manipulated. As a result, Christensen [1, Chapter 9] obtained instead of Eq. (12) the constitutive equation

$$\boldsymbol{\epsilon} = \mathbf{S} : \boldsymbol{\sigma} + \boldsymbol{\alpha} T, \tag{55}$$

where $\mathbf{S}$ is the compliance tensor of the material and $\boldsymbol{\alpha}$ is its coefficient of thermal-expansion second-order tensor. The entropy s in this case takes the form

$$\rho s = \boldsymbol{\alpha} : \boldsymbol{\sigma} + \rho c_p \frac{T}{T_R}, \tag{56}$$

where c_p is the specific heat at constant stress

$$c_p = T_R \left[\frac{\partial s}{\partial T} \right]_{\boldsymbol{\sigma}}. \tag{57}$$

The corresponding energy equation is given by

$$\rho c_p \frac{\partial T}{\partial t} + \nabla \cdot \mathbf{q} = -T_R \, \boldsymbol{\alpha} : \frac{\partial \boldsymbol{\sigma}}{\partial t}. \tag{58}$$

It can be shown that

$$\rho c_p - \rho c_v = T_R \, \boldsymbol{\alpha} : \mathbf{C} : \boldsymbol{\alpha}. \tag{59}$$

3.2 The homogenized energy equation

In the two-way TMC homogenization analysis both the displacements and the temperature deviation from a reference temperature are asymptotically expanded. The displacement-vector expansion is given by (cf. Eq. (1))

$$\mathbf{u}(\mathbf{x}, \mathbf{y}, t) = \mathbf{u}^0(\mathbf{x}, \mathbf{y}, t) + \delta \, \mathbf{u}^1(\mathbf{x}, \mathbf{y}, t) + \cdots, \tag{60}$$

which emphasizes the temporal dependence, whereas the temperature-deviation expansion has the form

$$T(\mathbf{x}, \mathbf{y}, t) = T^0(\mathbf{x}, \mathbf{y}, t) + \delta \, T^1(\mathbf{x}, \mathbf{y}, t) + \delta^2 \, T^2(\mathbf{x}, \mathbf{y}, t) + \cdots, \tag{61}$$

where the same periodicity conditions that were given by Eq. (3) hold for the coefficients $\mathbf{u}^{\xi}(\mathbf{x}, \mathbf{y}, t)$ and $T^{\xi}(\mathbf{x}, \mathbf{y}, t)$.

The heat flux $\mathbf{q}$ is given by Eq. (54) where as in Eq. (13),

$$\mathbf{k}(\mathbf{x}) = \mathbf{k}(\mathbf{y}). \tag{62}$$

By utilizing Eq. (4), the heat flux can be represented by

$$\mathbf{q} = \frac{1}{\delta}\mathbf{q}^0 + \mathbf{q}^1 + \delta \mathbf{q}^2 + O(\delta^2), \tag{63}$$

where

$$\mathbf{q}^0 = -\mathbf{k} \cdot \nabla_{\mathbf{y}} T^0, \quad \mathbf{q}^1 = -\mathbf{k} \cdot [\nabla_{\mathbf{x}} T^0 + \nabla_{\mathbf{y}} T^1], \quad \mathbf{q}^2 = -\mathbf{k} \cdot [\nabla_{\mathbf{x}} T^1 + \nabla_{\mathbf{y}} T^2]. \tag{64}$$

By substituting $\mathbf{q}$ in the energy equation (53) and using Eq. (4) and (7), we obtain the following relation

$$\rho c_v \frac{\partial}{\partial t}\left[T^0 + O(\delta)\right] + \left(\nabla_{\mathbf{x}} + \frac{1}{\delta}\nabla_{\mathbf{y}}\right) \cdot \left[\frac{1}{\delta}\mathbf{q}^0 + \mathbf{q}^1 + \delta \mathbf{q}^2 + O(\delta^2)\right] = -T_R \boldsymbol{\Gamma} : \frac{\partial}{\partial t}\left[\boldsymbol{\epsilon}^0_{\mathbf{x}} + \boldsymbol{\epsilon}^1_{\mathbf{x}} + O(\delta)\right]. \tag{65}$$

By equating terms of the order of $1/\delta^2$, we obtain

$$\nabla_{\mathbf{y}} \cdot \mathbf{q}^0 = 0. \tag{66}$$

It follows from the definition of $\mathbf{q}^0$ that $T^0 = T^0(\mathbf{x}, t)$ is independent of $\mathbf{y}$.

By equating terms of the order of $1/\delta$, we obtain

$$\nabla_{\mathbf{y}} \cdot \mathbf{q}^1 = 0. \tag{67}$$

The requirement that the temperature and normal heat-flux vector should be periodic on the RUC implies that (cf. Eqs. (20–25)):

$$T^1(y_1 = 0, t) = T^1(y_1 = D, t), \quad \mathbf{q}^1(y_1 = 0, t) \cdot \mathbf{e}_1 = \mathbf{q}^1(y_1 = D, t) \cdot \mathbf{e}_1, \tag{68,69}$$

$$T^1(y_2 = 0, t) = T^1(y_2 = H, t), \quad \mathbf{q}^1(y_2 = 0, t) \cdot \mathbf{e}_2 = \mathbf{q}^1(y_2 = H, t) \cdot \mathbf{e}_2, \tag{70,71}$$

$$T^1(y_3 = 0, t) = T^1(y_3 = L, t), \quad \mathbf{q}^1(y_3 = 0, t) \cdot \mathbf{e}_3 = \mathbf{q}^1(y_3 = L, t) \cdot \mathbf{e}_3. \tag{72,73}$$

In conjunction with the definition of $\mathbf{q}^1$, Eq. (67), together with the above periodicity requirements and that T^0 is independent of $\mathbf{y}$, forms a boundary-value problem over RUC for a prescribed $\nabla_{\mathbf{x}} T^0(\mathbf{x}, t)$. The solution of this problem yields

$$\nabla_{\mathbf{y}} T^1(\mathbf{x}, \mathbf{y}, t) = \tilde{\mathbf{A}}^k(\mathbf{y}) \cdot \nabla_{\mathbf{x}} T^0(\mathbf{x}, t). \tag{74}$$

Consequently, the total temperature gradient is given by

$$\nabla_{\mathbf{x}} T(\mathbf{x}, \mathbf{y}, t) = \nabla_{\mathbf{x}} T^0(\mathbf{x}, t) + \tilde{\mathbf{A}}^k(\mathbf{y}) \cdot \nabla_{\mathbf{x}} T^0(\mathbf{x}, t) = [\mathbf{I}_2 + \tilde{\mathbf{A}}^k(\mathbf{y})] \cdot \nabla_{\mathbf{x}} T^0(\mathbf{x}, t) \equiv \mathbf{A}^k(\mathbf{y}) \cdot \nabla_{\mathbf{x}} T^0(\mathbf{x}, t), \tag{75}$$

where $\mathbf{I}_2$ is the second-order unit tensor. The average of the total temperature gradient taken over the RUC is given by

$$\langle \nabla_{\mathbf{x}} T(\mathbf{x}, \mathbf{y}, t) \rangle = \frac{1}{V_y} \int_{V_y} \left[\nabla_{\mathbf{x}} T^0(\mathbf{x}, t) + \nabla_{\mathbf{y}} T^1(\mathbf{x}, \mathbf{y}, t) \right] \mathrm{d}V_y = \nabla_{\mathbf{x}} T^0(\mathbf{x}, t), \tag{76}$$

since the second term in the integral vanishes due to the periodicity of the temperature when employing the divergence theorem.

The heat flux $\mathbf{q}$ is given according to Eqs. (63), (64) and (75) by

$$\mathbf{q} = \mathbf{q}^1 + O(\delta) = -\mathbf{k}(\mathbf{y}) \cdot \mathbf{A}^k(\mathbf{y}) \cdot \nabla_{\mathbf{x}} T^0(\mathbf{x}, t) + O(\delta). \tag{77}$$

Hence the average of the heat flux $\bar{\mathbf{q}}$ over the RUC is given by

$$\bar{\mathbf{q}} = -\mathbf{k}^* \cdot \nabla_{\mathbf{x}} T^0(\mathbf{x}, t), \tag{78}$$

where $\mathbf{k}^*$ is the effective conductivity second-order tensor defined by

$$\mathbf{k}^* = \frac{1}{V_y} \int_{V_y} \mathbf{k}(\mathbf{y}) \cdot \mathbf{A}^k(\mathbf{y}) \mathrm{d}V_y. \tag{79}$$

In the framework of the HFGMC model, the corresponding effective conductivity matrix can be computed from Eq. (79) by changing the integration operation into a summation over the subcells (cf. Eq. (42)).

Finally, by equating terms of the order of δ^0 in Eq. (65), the following equality holds

$$\rho c_v \frac{\partial}{\partial t} T^0(\mathbf{x}, t) + \nabla_{\mathbf{x}} \cdot \mathbf{q}^1 + \nabla_{\mathbf{y}} \cdot \mathbf{q}^2 = -T_R \boldsymbol{\Gamma}(\mathbf{y}) : \frac{\partial}{\partial t} \left[\boldsymbol{\epsilon}^0_{\mathbf{x}}(\mathbf{x}, t) + \boldsymbol{\epsilon}^1_{\mathbf{y}}(\mathbf{x}, \mathbf{y}, t) \right]. \tag{80}$$

By employing Eq. (28), Eq. (80) takes the form

$$\left[\rho c_v + T_R \boldsymbol{\Gamma}(\mathbf{y}) : \mathbf{A}^T(\mathbf{y}) \right] \frac{\partial}{\partial t} T^0(\mathbf{x}, t) + \nabla_{\mathbf{x}} \cdot \mathbf{q}^1 + \nabla_{\mathbf{y}} \cdot \mathbf{q}^2 = -T_R \boldsymbol{\Gamma}(\mathbf{y}) : \mathbf{A}^M(\mathbf{y}) : \frac{\partial}{\partial t} \bar{\boldsymbol{\epsilon}}(\mathbf{x}, t). \tag{81}$$

By taking the average of Eq. (81) over the RUC, the following average energy equation results:

$$(\rho c_v)^* \frac{\partial}{\partial t} T^0(\mathbf{x}, t) - \mathbf{k}^* \nabla^2_{\mathbf{x}} T^0(\mathbf{x}, t) = -T_R \boldsymbol{\Gamma}^* : \frac{\partial}{\partial t} \bar{\boldsymbol{\epsilon}}(\mathbf{x}, t), \tag{82}$$

where the effective value of ρc_v is defined by

$$(\rho c_v)^* = \overline{\rho c_v} + \frac{T_R}{V_y}\int_{V_y} \mathbf{\Gamma}(\mathbf{y}) : \mathbf{A}^T(\mathbf{y})\, \mathrm{d}V_y \tag{83}$$

with $\overline{\rho c_v}$ being the average of ρc_v over the RUC. In establishing Eq. (82), Eqs. (77–78) have been utilized and Levin's result, Eq. (33), has been used to identify $\mathbf{\Gamma}^*$. In addition, the average of $\nabla_{\mathbf{y}} \cdot \mathbf{q}^2$ vanishes because the divergence theorem gives

$$\frac{1}{V_y}\int_{V_y} \nabla_{\mathbf{y}} \cdot \mathbf{q}^2 \mathrm{d}V_y = \frac{1}{\Gamma_y}\int_{\Gamma_y} \mathbf{q}^2 \cdot \mathbf{n}\, \mathrm{d}\Gamma_y = 0, \tag{84}$$

since the periodicity of the temperature causes $\mathbf{q}^2$ to be periodic and contributions from opposite sides on the boundary of the RUC ($\mathbf{n}$ is the normal to its surface Γ_y) cancel each other.

The corresponding homogenized constitutive equation can be easily established by employing the appropriate expansions in Eq. (12). As a result, the strong form of the equilibrium equation can be easily shown to yield Eq. (19) but with the prescribed constant temperature in the one-way TMC replaced here by the temperature T^0. The resulting global constitutive equation is given by

$$\bar{\boldsymbol{\sigma}} = \mathbf{C}^* : \bar{\boldsymbol{\epsilon}} - \mathbf{\Gamma}^*\, T^0. \tag{85}$$

This equation is the counterpart of Eq. (30) where the prescribed constant temperature in the one-way TMC in the latter is replaced here by the temperature T^0 which is governed by the coupled homogenized energy equation (82).

In order to establish the homogenized energy equation that corresponds to (58), the following relation that expresses the stress at a point in the RUC in terms of the global stress and temperature, is employed:

$$\boldsymbol{\sigma}(\mathbf{x}, \mathbf{y}, t) = \mathbf{B}^M(\mathbf{y}) : \bar{\boldsymbol{\sigma}}(\mathbf{x}, t) + \mathbf{B}^T(\mathbf{y})\, T^0(\mathbf{x}, t), \tag{86}$$

where $\mathbf{B}^M$ and $\mathbf{B}^T$ are referred to as mechanical and thermal-stress concentration tensors, respectively. By employing Eq. (28) (with T replaced by T^0) and (85), we obtain the following expressions for these tensors in terms of the mechanical $\mathbf{A}^M$ and thermal $\mathbf{A}^T$ strain-concentration tensors

$$\mathbf{B}^M = \mathbf{C}\,\mathbf{A}^M\,[\mathbf{C}^*]^{-1}, \quad \mathbf{B}^T = \mathbf{C}\,\mathbf{A}^M\boldsymbol{\alpha}^* + \mathbf{C}\,\mathbf{A}^T - \mathbf{\Gamma}. \tag{87, 88}$$

Consequently, by homogenizing the energy equation (58) and using the above expressions (87)–(88) in conjunction with Eq. (33), the following energy equation is obtained

$$(\rho c_p)^* \frac{\partial}{\partial t} T^0(\mathbf{x}, t) - \mathbf{k}^* \nabla_{\mathbf{x}}^2 T^0(\mathbf{x}, t) = -T_R \boldsymbol{\alpha}^* : \frac{\partial}{\partial t}\bar{\boldsymbol{\sigma}}(\mathbf{x}, t), \tag{89}$$

where the effective value of ρc_p is defined by

$$(\rho c_p)^* = \overline{\rho c_p} + \frac{T_R}{V_y}\int_{V_y} \boldsymbol{\alpha}(\mathbf{y}) : \mathbf{B}^T(\mathbf{y})\, \mathrm{d}V_y \tag{90}$$

with $\overline{\rho c_p}$ being the average of ρc_p over RUC. In the framework of the HFGMC model, the corresponding effective values: $(\rho c_v)^*$ and $(\rho c_p)^*$ can be readily computed from Eq. (83) and (90) by changing the integration operation into summations over the subcells.

It has already been observed that the solution of the homogenized energy equations (82) and (89), which is actually based on the one-way TMC problem, provides, in conjunction with the effective properties of the homogenized material, the smeared temperature $T^0(\mathbf{x}, t)$ which is independent of the location $\mathbf{y}$ within the RUC. Thus, this solution forms a representative value of the actual temperature variations within RUC caused by a far-field mechanical loading. Furthermore, the temperature field is determined from the homogenized energy equations under a steady-state condition such that the term that involves the effective thermal conductivity vanishes. Consequently, the temperature field $T^0(\mathbf{x}, t)$ that is determined from the energy equation is not based upon the enforcement of the continuity of temperature and heat-flux conditions between the constituents of the multiphase composite.

In the next section, the TMC equations in each constituent of the multiphase composite are considered in conjunction with the micromechanical analysis. As a result, the detailed variation of the temperature in the RUC (just

like the mechanical field in the one-way TMC) is obtained. However, if a representative value of the temperature only is sought, the resulting field variables obtained from a one-way TMC can be employed to solve Eq. (82) or (89) without the need to perform the full two-way TMC micromechanical analysis that is described in the following section.

We conclude this section by noting that, in the presence of inelastic effects, the corresponding homogenized energy equations take the form

$$(\rho c_v)^* \dot{T}^0(\mathbf{x},t) - \mathbf{k}^* \nabla^2_{\mathbf{x}} T^0(\mathbf{x},t) = \zeta \bar{\boldsymbol{\sigma}}(\mathbf{x},t) : \dot{\bar{\boldsymbol{\epsilon}}}^I(\mathbf{x},t) - T_R \boldsymbol{\Gamma}^* : \left[\dot{\bar{\boldsymbol{\epsilon}}}(\mathbf{x},t) - \dot{\bar{\boldsymbol{\epsilon}}}^I(\mathbf{x},t)\right], \tag{91}$$

$$(\rho c_p)^* \dot{T}^0(\mathbf{x},t) - \mathbf{k}^* \nabla^2_{\mathbf{x}} T^0(\mathbf{x},t) = \zeta \bar{\boldsymbol{\sigma}}(\mathbf{x},t) : \dot{\bar{\boldsymbol{\epsilon}}}^I(\mathbf{x},t) - T_R \boldsymbol{\alpha}^* : \left[\dot{\bar{\boldsymbol{\sigma}}}(\mathbf{x},t) - \dot{\bar{\boldsymbol{\sigma}}}^I(\mathbf{x},t)\right], \tag{92}$$

where $\bar{\boldsymbol{\sigma}}^I$ and $\bar{\boldsymbol{\epsilon}}^I$ are the global inelastic stress and strain of the composite. In addition, the rate of the global inelastic work $\dot{\overline{W}}_I = \bar{\boldsymbol{\sigma}} : \dot{\bar{\boldsymbol{\epsilon}}}^I$ is usually multiplied by a partition factor ζ to indicate that only a portion of the inelastic work (about 90%) is transformed into heat [20, Chapter 16]. Equation (91) coincides with the energy equation which is given by Allen [21] for a homogeneous inelastic anisotropic material. In [22], the homogenized energy equation (91), in conjunction with the older method of cells micromechanical analysis, was employed to investigate the inelastic response and buckling of metal-matrix composite plates.

3.3 Solution of the repeating-unit-cell problem with full TMC

The HFGMC micromechanical model which is extended herein to a two-way TMC is employed to predict the fully coupled thermo-inelastic behavior of triply periodic composites.

The local (subcell) constitutive equation of the material which, in general, is assumed to be thermo-inelastic is given (cf. Eq. (34)), in matrix notation, by

$$\boldsymbol{\sigma}^{(\alpha\beta\gamma)} = \mathbf{C}^{(\alpha\beta\gamma)} \boldsymbol{\epsilon}^{(\alpha\beta\gamma)} - \boldsymbol{\Gamma}^{(\alpha\beta\gamma)} T^{(\alpha\beta\gamma)} - \boldsymbol{\sigma}^{I(\alpha\beta\gamma)}. \tag{93}$$

It should be emphasized that $T^{(\alpha\beta\gamma)}$ denotes, in the present two-way TMC coupling formulation, the unknown temperature deviation in subcell $(\alpha\beta\gamma)$ from a reference temperature. The equilibrium equation in subcell $(\alpha\beta\gamma)$ is given by Eq. (19) which also includes the inelastic stress, and where all field variables are labeled by $(\alpha\beta\gamma)$. The associated energy equation that governs the material behavior in subcell $(\alpha\beta\gamma)$ is given by

$$\rho c_v \dot{T}^{(\alpha\beta\gamma)} + \mathbf{q}^{(\alpha\beta\gamma)} = \zeta \boldsymbol{\sigma}^{(\alpha\beta\gamma)} \dot{\boldsymbol{\epsilon}}^{I(\alpha\beta\gamma)} - T_R \boldsymbol{\Gamma}^{(\alpha\beta\gamma)} \left[\dot{\boldsymbol{\epsilon}}^{(\alpha\beta\gamma)} - \dot{\boldsymbol{\epsilon}}^{I(\alpha\beta\gamma)}\right]. \tag{94}$$

For inelastic isotropic materials in which the inelastic flow is incompressible, we have

$$T_R \boldsymbol{\Gamma}^{(\alpha\beta\gamma)} \left[\dot{\boldsymbol{\epsilon}}^{(\alpha\beta\gamma)} - \dot{\boldsymbol{\epsilon}}^{I(\alpha\beta\gamma)}\right] = T_R \boldsymbol{\Gamma}^{(\alpha\beta\gamma)} \dot{\boldsymbol{\epsilon}}^{(\alpha\beta\gamma)}, \tag{95}$$

As is shown in the following, the spatial derivatives in Eq. (94) can be eliminated. As a result, this equation is reduced to an ordinary differential equation in time. Consequently, let us represent it in the following compact form

$$[M]^{(\alpha\beta\gamma)} \dot{T}^{(\alpha\beta\gamma)} = [S]^{(\alpha\beta\gamma)} T^{(\alpha\beta\gamma)} + [\dot{Q}]^{(\alpha\beta\gamma)}, \tag{96}$$

where $[\dot{Q}]^{(\alpha\beta\gamma)}$ denotes the right-hand side of Eq. (94). The implicit difference in time of Eq. (96) yields [23, Chapter 6]

$$\left\{[M]^{(\alpha\beta\gamma)} - \omega \Delta t [S]^{(\alpha\beta\gamma)}\right\} T^{(\alpha\beta\gamma)}_{n+1} = \left\{[M]^{(\alpha\beta\gamma)} + (1-\omega)\Delta t [S]^{(\alpha\beta\gamma)}\right\} T^{(\alpha\beta\gamma)}_{n} + [Q]^{(\alpha\beta\gamma)}_{n} - [Q]^{(\alpha\beta\gamma)}_{n-1}, \tag{97}$$

where $\Delta t = t_{n+1} - t_n$ and ω is a parameter (for the Crank–Nicolson scheme: $\omega = 1/2$).

As in the one-way TMC micromechanical analysis, the basic assumption in the HFGMC model with two-way TMC is that the displacement vector $\mathbf{u}^{(\alpha\beta\gamma)}$ in each subcell is expanded into quadratic form in terms of its local

coordinates $(\bar{y}_1^{(\alpha)}, \bar{y}_2^{(\beta)}, \bar{y}_3^{(\gamma)})$, as was given by Eq. (35). Similarly, the unknown temperature deviation $T^{(\alpha\beta\gamma)}$ in the subcell is also expanded as follows:

$$T^{(\alpha\beta\gamma)} = T_{(000)}^{(\alpha\beta\gamma)} + \bar{y}_1^{(\beta)} T_{(100)}^{(\alpha\beta\gamma)} + \bar{y}_2^{(\beta)} T_{(010)}^{(\alpha\beta\gamma)} + \bar{y}_3^{(\gamma)} T_{(001)}^{(\alpha\beta\gamma)} + \frac{1}{2}(3\bar{y}_1^{(\alpha)2} - \frac{d_\alpha^2}{4}) T_{(200)}^{(\alpha\beta\gamma)} + \frac{1}{2}\left(3\bar{y}_2^{(\beta)2} - \frac{h_\beta^2}{4}\right) T_{(020)}^{(\alpha\beta\gamma)} + \frac{1}{2}\left(3\bar{y}_3^{(\gamma)2} - \frac{l_\gamma^2}{4}\right) T_{(002)}^{(\alpha\beta\gamma)}, \tag{98}$$

where $T_{(000)}^{(\alpha\beta\gamma)}$ is the volume-averaged temperature and the higher-order terms $T_{(lmn)}^{(\beta\gamma)}$ are additional unknowns.

The unknown terms $\mathbf{W}_{(lmn)}^{(\alpha\beta\gamma)}$ and $T_{(lmn)}^{(\alpha\beta\gamma)}$ are determined from the fulfillment of the aforementioned coupled equilibrium and energy equations, the periodic boundary conditions, Eqs. (20–25) and Eqs. (68–73), and the interfacial continuity conditions of displacements, tractions, temperatures and heat fluxes between adjacent subcells. As in the one-way TMC micromechanical analysis, the principal ingredient in the present micromechanical analysis is that all these conditions are imposed in an average (integral) sense.

As a result of the imposition of these conditions, a linear system of algebraic equations at the current time step is obtained which can be also represented by Eq. (36). Here, the displacement-temperature vector $\mathbf{U}$ contains the unknown displacement and temperature which has the form (37), but in subcell $(\alpha\beta\gamma)$ these coefficients, which appear on the right-hand side of Eqs. (35) and (98), are

$$\mathbf{U}^{(\alpha\beta\gamma)} = \left[\mathbf{W}_{(000)}, T_{(000)}, \mathbf{W}_{(100)}, T_{(100)}, \mathbf{W}_{(010)}, T_{(010)}, \mathbf{W}_{(001)}, T_{(001)}, \mathbf{W}_{(200)}, T_{(200)}, \mathbf{W}_{(020)}, T_{(020)}, \mathbf{W}_{(002)}, T_{(002)}\right]^{(\alpha\beta\gamma)}. \tag{99}$$

The solution of Eq. (36) at a given time step enables the establishment of the following localization relation which expresses the average strain $\bar{\boldsymbol{\epsilon}}^{(\alpha\beta\gamma)}$ and temperature $\bar{T}^{(\alpha\beta\gamma)}$ in the subcell $(\alpha\beta\gamma)$ to the externally applied average strain $\bar{\boldsymbol{\epsilon}}$ in the form:

$$\begin{Bmatrix} \bar{\boldsymbol{\epsilon}}^{(\alpha\beta\gamma)} \\ \bar{T}^{(\alpha\beta\gamma)} \end{Bmatrix} = \begin{Bmatrix} \mathbf{A}^{M(\alpha\beta\gamma)} \\ \mathbf{A}^{T(\alpha\beta\gamma)} \end{Bmatrix} \bar{\boldsymbol{\epsilon}} + \begin{Bmatrix} \mathbf{V}^{T(\alpha\beta\gamma)} \\ v^{T(\alpha\beta\gamma)} \end{Bmatrix} + \begin{Bmatrix} \mathbf{V}^{I(\alpha\beta\gamma)} \\ v^{I(\alpha\beta\gamma)} \end{Bmatrix}, \tag{100}$$

where $\mathbf{A}^{M(\alpha\beta\gamma)}$ and $\mathbf{A}^{T(\alpha\beta\gamma)}$ are the new mechanical and thermal concentration matrices of subcell $(\alpha\beta\gamma)$ of the present two-way micromechanical analysis; $\mathbf{V}^{T(\alpha\beta\gamma)}$ and $\mathbf{V}^{I(\alpha\beta\gamma)}$ are matrices that involve thermal and inelastic effects in the subcell, and $v^{T(\alpha\beta\gamma)}$ and $v^{I(\alpha\beta\gamma)}$ are the corresponding scalars. These thermal and inelastic matrices and the corresponding scalars arise due to the existence of $[Q]_n^{(\alpha\beta\gamma)}$ and $[Q]_{n-1}^{(\alpha\beta\gamma)}$ in Eq. (97) at the previous time steps. It should be noted that, in the present case of two-way TMC, the application of the far-field strain $\bar{\boldsymbol{\epsilon}}$ induces a temperature deviation $T^{(\alpha\beta\gamma)}$ from the reference temperature in the subcell.

In order to establish the global (macroscopic) constitutive equation of the composite, we utilize the definition of the average stress in the composite in terms of average stress in the subcells; see Eq. (40). By substituting Eqs. (93) and (100) in (40), one obtains the final form of the effective constitutive law of the multiphase fully coupled thermo-inelastic composite, which relates the average stress $\bar{\boldsymbol{\sigma}}$, strain $\bar{\boldsymbol{\epsilon}}$, thermal stress $\bar{\boldsymbol{\sigma}}^T$ and inelastic stress $\bar{\boldsymbol{\sigma}}^I$ as follows:

$$\bar{\boldsymbol{\sigma}} = \mathbf{C}^* \, \bar{\boldsymbol{\epsilon}} - (\bar{\boldsymbol{\sigma}}^T + \bar{\boldsymbol{\sigma}}^I). \tag{101}$$

In this equation $\mathbf{C}^*$ is the effective stiffness matrix which is given by

$$\mathbf{C}^* = \frac{1}{DHL} \sum_{\alpha=1}^{N_\alpha} \sum_{\beta=1}^{N_\beta} \sum_{\gamma=1}^{N_\gamma} d_\alpha h_\beta l_\gamma \left[\mathbf{C}^{(\alpha\beta\gamma)} \mathbf{A}^{M(\alpha\beta\gamma)} - \Gamma^{(\alpha\beta\gamma)} \mathbf{A}^{T(\alpha\beta\gamma)}\right]. \tag{102}$$

As in the one-way TMC analysis, the symmetry of $\mathbf{C}^*$ can be verified by considering in this case the first term in the RHS of Eq. (100). The global thermal stress $\bar{\boldsymbol{\sigma}}^T$ is determined from

$$\bar{\boldsymbol{\sigma}}^T = -\frac{1}{DHL} \sum_{\alpha=1}^{N_\alpha} \sum_{\beta=1}^{N_\beta} \sum_{\gamma=1}^{N_\gamma} d_\alpha h_\beta l_\gamma \left[\mathbf{C}^{(\alpha\beta\gamma)} \mathbf{V}^{T(\alpha\beta\gamma)} - \boldsymbol{\Gamma}^{(\alpha\beta\gamma)} v^{T(\alpha\beta\gamma)}\right]. \tag{103}$$

The global inelastic stress $\bar{\boldsymbol{\sigma}}^I$ is of the from

$$\bar{\boldsymbol{\sigma}}^I = -\frac{1}{DHL}\sum_{\alpha=1}^{N_\alpha}\sum_{\beta=1}^{N_\beta}\sum_{\gamma=1}^{N_\gamma} d_\alpha h_\beta l_\gamma \left[\mathbf{C}^{(\alpha\beta\gamma)}\mathbf{V}^{I(\alpha\beta\gamma)} - \boldsymbol{\Gamma}^{(\alpha\beta\gamma)} v^{I(\alpha\beta\gamma)} - \bar{\boldsymbol{\sigma}}^{I(\alpha\beta\gamma)}\right]. \tag{104}$$

The average of the temperature deviation from T_R over the RUC, which is predicted from the two-way micromechanics analysis, is given by

$$\bar{T} = \frac{1}{DHL}\sum_{\alpha=1}^{N_\alpha}\sum_{\beta=1}^{N_\beta}\sum_{\gamma=1}^{N_\gamma} d_\alpha h_\beta l_\gamma \bar{T}^{(\alpha\beta\gamma)}, \tag{105}$$

where $\bar{T}^{(\alpha\beta\gamma)}$ is the average temperature deviation in the subcell. In the following section the predicted temperature average $\bar{T}$ over the RUC will be compare with T^0 that is calculated from the homogenized energy equation (91). As stated before, this energy equation involves the homogenized field variables and the effective composite's parameters computed from the one-way micromechanics analysis in which, in particular, continuity of the temperature and heat fluxes is not imposed. For homogeneous (unreinforced) materials, $\bar{T}$ coincides, as is expected, with T^0.

4 Applications

The established two-way TMC HFGMC micromechanics analysis is applied here to predict the behavior of Al_2O_3 continuous reinforced composites in various circumstances. Two types of matrices are chosen to illustrate the composites' responses. In the first case an aluminum alloy is chosen as a matrix. In this case the inelastic effects of the metallic matrix are involved in its energy equation (94). In the second type, a polymeric matrix (epoxy) is chosen. Here, the TMC arises due to the existence of the total strain rates in Eq. (94) only. The material properties of the Al_2O_3 fibers and the aluminum and epoxy matrices are given in Tables 1–3. The RUC, Fig. 1(b), in which the continuous fiber is oriented in the y_1-direction, has been divided into 32×32 subcells in order to model a circular fiber cross-section with sufficient accuracy. In all cases the volume fraction of the Al_2O_3 fibers is 0.3 and the rate of applied strain is $1\ s^{-1}$.

The standard thermomechanical coupling coefficient in thermoelastic materials is given by

$$\delta_1 = \frac{E(1+\nu)\alpha^2 T_R}{(1-2\nu)(1-\nu)\rho c_v}, \tag{106}$$

where E and ν are the Young's modulus and Poisson's ratio of the material, respectively. This parameter characterizes the amount of thermomechanical coupling in these material (i.e., the coupling that is caused by the total

Table 1 Elastic and thermal parameters of the isotropic Al_2O_3 fibers

E(GPa)	ν	α (10^{-6}/K)	k (W/(m K))	ρc_v (M J/(m^3 K))
400	0.24	16.3	30	3.1

E, ν, α, k and ρc_v denote the Young's modulus, Poisson's ratio, coefficient of thermal expansion, thermal conduction and heat capacity, respectively

Table 2 Elastic, plastic and thermal parameters of the isotropic elastoplastic aluminum matrix

E(GPa)	ν	α (10^{-6}/K)	σ_y (MPa)	E_s (GPa)	k (W/(m K))	ρc_v (M J/(m^3 K))
72.4	0.33	22.5	371.5	23	116.7	2.25

E, ν, α, σ_y, E_s, k and ρc_v denote the Young's modulus, Poisson's ratio, coefficient of thermal expansion, yield stress, secondary modulus, thermal conduction and heat capacity, respectively

Table 3 Elastic and thermal parameters of the isotropic epoxy-polymeric matrix

E(GPa)	ν	α (10^{-6}/K)	k (W/(m K))	ρc_v (M J/(m^3 K))
3.45	0.35	54	0.18	1.28

E, ν, α, k and ρc_v denote the Young's modulus, Poisson's ratio, coefficient of thermal expansion, thermal conduction and heat capacity, respectively

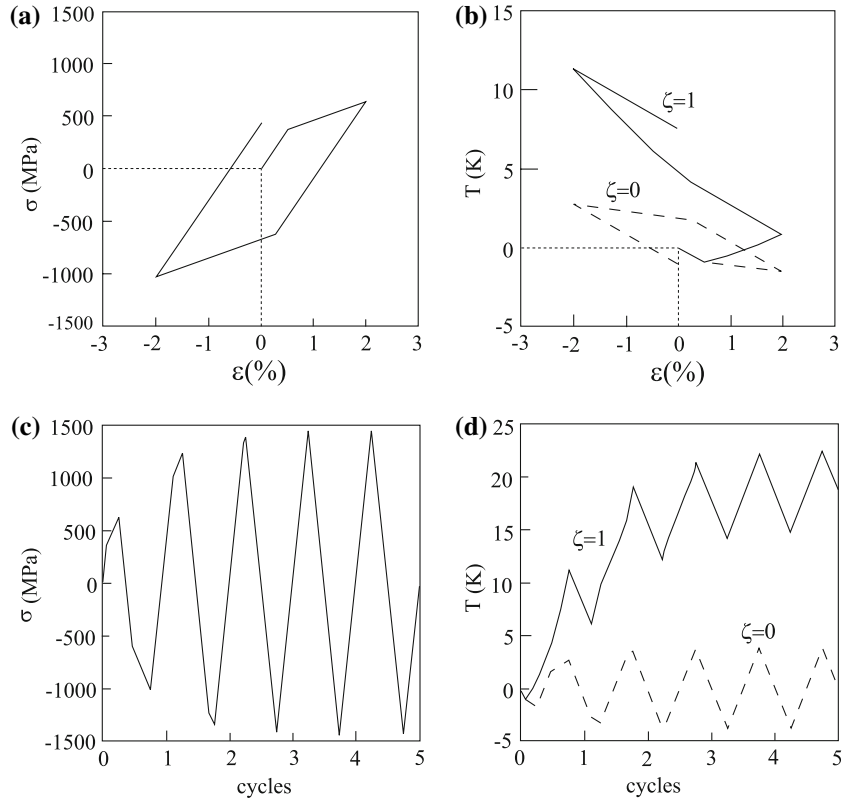

Fig. 2 (**a**) The uniaxial stress–strain response in one cycle of the unreinforced aluminum and, (**b**) the resulting induced temperature deviation when $\zeta = 1$ and 0 in Eq. (94). (**c**) The uniaxial response of the aluminum matrix in five cycles and, (**d**) the resulting induced average temperature deviation when $\zeta = 1$ and 0

strain-rate term in Eq. (94) but without including the inelastic effects). The values of thermomechanical coupling coefficient δ_1 of the monolithic Al_2O_3 fibers, aluminum and epoxy matrices are: $\delta_1 = 0.031$, 0.027 and 0.016, respectively. Thus, the fibers exhibit the highest value, while the epoxy has the lowest value. However, due to the existence of the inelastic effects in the aluminum matrix, this material exhibits a very strong TMC as is discussed below.

It is instructive to exhibit the behavior of the unreinforced aluminum and the induced temperature deviation during a cyclic uniaxial stress loading to a maximum strain of $\mp 2\%$ in two different cases. To this end, Figs. 2(a) and (b), show the resulting stress and the induced temperature deviation when in Eq. (94) $\zeta = 1$ and $\zeta = 0$. In the first case full TMC is taken into account, while in the second case the heat generated by the rate of inelastic work, $\dot{W}_I^{(\alpha\beta\gamma)} = \boldsymbol{\sigma}^{(\alpha\beta\gamma)} : \dot{\boldsymbol{\epsilon}}^{I(\alpha\beta\gamma)}$, is neglected, while retaining the coupling caused by the term $T_R \boldsymbol{\Gamma}^{(\alpha\beta\gamma)} : \dot{\boldsymbol{\epsilon}}^{(\alpha\beta\gamma)}$ that represents the total strain rate in this equation (which is accounted for by the coupling coefficient δ_1). Figures 2(a) and (b) clearly show that the heat generated by the rate of plastic work is predominant. Except in Fig. (2), ζ is taken in all cases to be equal to 1. The effect of TMC on the stress–strain response is negligibly small. Indeed, under a

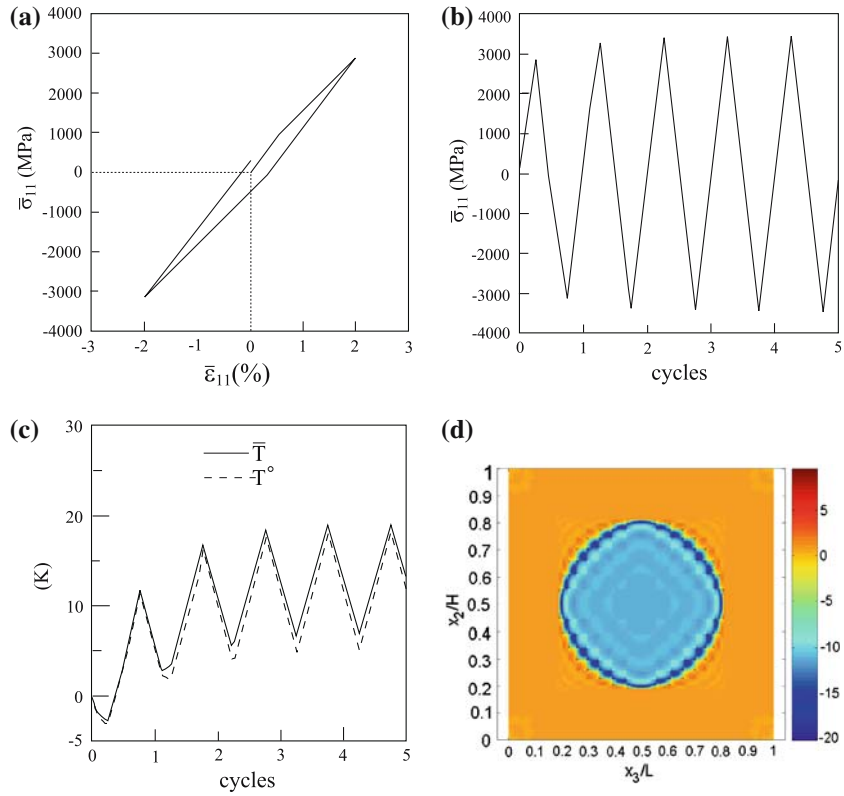

Fig. 3 (**a**) The uniaxial stress–strain response in one cycle of the Al_2O_3/aluminum composite loaded in the fiber direction. (**b**) The uniaxial response of the Al_2O_3/aluminum composite in five cycles loaded in the fibers direction and, (**c**) the resulting induced average temperature deviations $\bar{T}$ and T^0 as predicted by the two-way TMC, Eq. (105), and the homogenized energy equation (91), respectively. (**d**) Surface plot of the temperature-deviation variation in the RUC at $\bar{\epsilon}_{11} = 0.02$

uniaxial stress loading at a strain of $\epsilon = 2\%$, the resulting thermal stress is $\sigma^T = 3.5\,\mathrm{MPa}$ as against inelastic stress of $\sigma^I = 616\,\mathrm{MPa}$, thus forming a stress of $\sigma = 631\,\mathrm{MPa}$.

The effect of the TMC caused by the inelastic effects of the unreinforced aluminum can be further observed when this material is subjected to five complete cycles of uniaxial stress loading–unloading to a maximum strain amplitude of $\mp 2\%$. The response of the material and the induced temperature deviation due to the two-way TMC are shown in Figs. 2(c) and (d). Here, too, the effect of TMC on the resulting stress is negligible but the induced temperature deviation is significant.

Consider next an Al_2O_3/aluminum continuous reinforced composite which is loaded in the 1-direction parallel to the fibers. Its global stress–strain response in one complete cycle of loading–unloading is shown in Fig. 3(a). As can be expected, the effect of the fiber is dominant in this type of loading. Figures 3(b) and (c) exhibit the behavior of this composite under five cycles of loading–unloading to a maximum strain amplitude $|\bar{\epsilon}_{11}| = 0.02$. In both Figs. 3(a) and (b) the effect of TMC on the axial stress is negligible (just like the unreinforced aluminum), but the induced temperature deviation caused by this coupling is significant. This is shown in Fig. 3(c) where the induced average temperature deviation $\bar{T}$, computed from Eq. (105), which is based on the two-way TMC, and the induced temperature deviation T^0, which is directly obtained from integrating the homogenized energy equation (91), are exhibited. It is clearly seen that both curves are quite close in this case. Figure 3(d) presents a surface plot of the temperature deviation distribution in the RUC of the composite that is loaded to a strain of $\bar{\epsilon}_{11} = 2\%$. It is seen that the temperature deviation varies between 10 K and -20 K. These values are significant and therefore, the information provided by the homogenized energy equation: $T^0 = -3\,\mathrm{K}$ at this strain is not useful as long as one is looking for

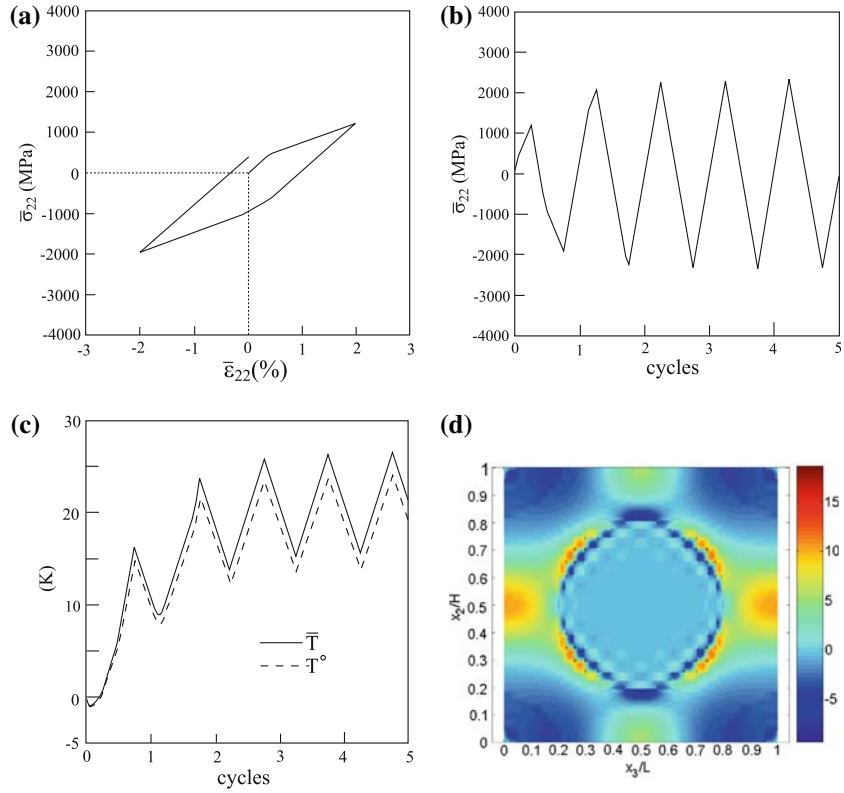

Fig. 4 (**a**) The uniaxial stress–strain response in one cycle of the Al_2O_3 /aluminum composite loaded in the transverse direction to the fibers. (**b**) The uniaxial response of the Al_2O_3/aluminum composite in five cycles loaded in the transverse direction to the fibers and, (**c**) the resulting induced average temperature deviations $\bar{T}$ and T^0 as predicted by the two-way TMC, Eq. (105), and the homogenized energy equation (91), respectively. (**d**) Surface plot of the temperature-deviation variation in the RUC at $\bar{\epsilon}_{22} = 0.02$

critical hot spots in the composite where failure may take place. Thus, a two-way TMC micromechanical analysis in such cases is necessary. It should be mentioned that, in contrast to the case of one-way TMC, $\bar{\sigma}^T_{11} \neq \Gamma^*_{11} T^0$ in the present case of two-way TMC.

Figure 4(a) shows the global stress–strain curve in one cycle of the Al_2O_3/aluminum unidirectional composite that is loaded in the transverse 2-direction. By comparing this figure with Fig. 3(a), one can readily observe the appreciable inelastic flow of the aluminum matrix. Figures 4(b) and (c) show the transverse response of the composite to five cycles of loading–unloading of the composite up to $|\bar{\epsilon}_{22}| = 0.02$ and the resulting induced temperature deviations $\bar{T}$ and T^0 which are quite close to each other. In Fig. 4(d), a surface plot of the temperature deviation distribution at $\bar{\epsilon}_{22} = 2\%$ is shown. Here, the temperature deviation varies between 20 K and -10 K whereas the homogenized energy equation merely provides that $T^0 = 0.6$ K. Here too, $\bar{\sigma}^T_{22} \neq \Gamma^*_{22} T^0$ in the present case of two-way TMC, which is in contrast to the situation in one-way TMC.

In Figs. 5 and 6, the behavior of the unidirectional Al_2O_3/aluminum composite under transverse-shear $\bar{\epsilon}_{23}$ and axial-shear $\bar{\epsilon}_{12}$ loadings of one and five cycles are shown. In Fig. 5, the maximum applied transverse-shear strain is $|\bar{\epsilon}_{23}| = 0.02$, whereas in Fig. 6 the maximum value of the applied axial-shear strain is $|\bar{\epsilon}_{12}| = 0.02$. In particular, Figs. 5(c) and 6(c) exhibit the induced temperature deviations as predicted from the two-way micromechanical analysis and the homogenized energy equation when the Al_2O_3/aluminum unidirectional composite is subjected to five cycles of transverse-shear and axial-shear loading, respectively. These figures show that the induced temperature deviations are significant in both types of applied shear loadings. These temperatures are caused by the two-way TMC in conjunction with the inelastic effects of the aluminum matrix. Such induced temperatures are, of course, absent in a one-way TMC analysis. They are also absent in the case of polymeric matrices in which

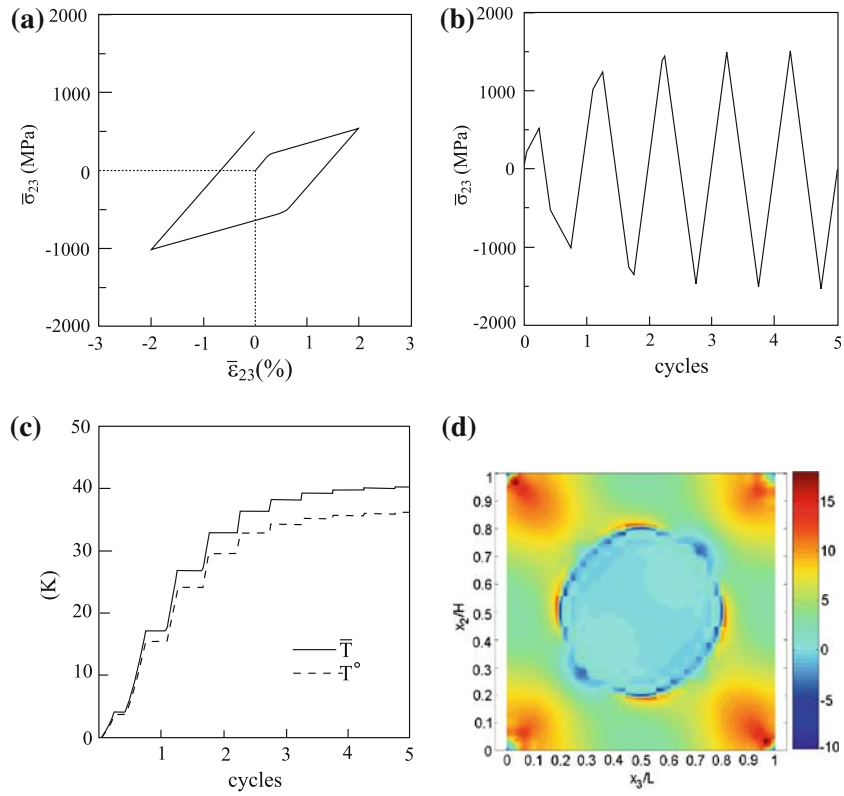

Fig. 5 The transverse shear stress–strain response in: (**a**) one cycle and, (**b**) five cycles of the Al_2O_3/aluminum composite. (**c**) The average temperature deviations $\bar{T}$ and T^0 as predicted by the two-way TMC, Eq. (105), and the homogenized energy equation (91), respectively, which are induced by a transverse shear loading of the composite to a strain of $\bar{\epsilon}_{23} = 0.02$. (**d**) Surface plot of the temperature deviation variation in the RUC at $\bar{\epsilon}_{23} = 0.02$

inelastic effects do not exist. The surface plots of the induced temperature deviation distributions that correspond to an applied transverse shear of $\bar{\epsilon}_{23} = 0.02$ and applied axial-shear strain of $\bar{\epsilon}_{12} = 0.02$ are presented in Figs. 5(d) and 6(d), respectively. The corresponding temperature deviations to Figs. 5(d) and 6(d) that are predicted by the homogenized energy equation (91) are $T^0 = 3.7\,\mathrm{K}$ and $T^0 = 4\,\mathrm{K}$, respectively, indicating again that these predictions are not useful in predicting hot spots in the composite. In both types of shear loadings, $\bar{\sigma}^T_{23} = \bar{\sigma}^T_{12} = 0$ as well as $\mathbf{\Gamma}^*_{23} = \mathbf{\Gamma}^*_{12} = 0$.

Thus far the two-way TMC micromechanical analysis has been applied on metal-matrix composites. Let us consider a polymeric matrix composite, namely Al_2O_3/epoxy. Here the ratios $T^0/\bar{T}$ between the induced temperature deviations caused by the two-way TMC as predicted from Eqs. (91) and (105) are 1.6 K and 0.7 K for normal loading in the axial and transverse directions, respectively. Thus, the correspondence between the predictions of these equations is no longer close as in the previous case of metal-matrix composite. This is attributed to the higher contrast of between the Young's moduli of the Al_2O_3 fibers and the epoxy matrix rendering the homogenized energy equation less useful, even for the prediction of the induced average temperature. In addition, a careful check of the induced temperature-deviation distributions in the composite reveals again that the homogenized-energy-equation prediction is not representative of the actual temperature variations as in the previously discussed cases.

5 Conclusions

In order to describe and predict the response of a multiphase composite that consists of several phases, an appropriate micromechanical analysis should be established that takes into account the behavior of the individual constituents

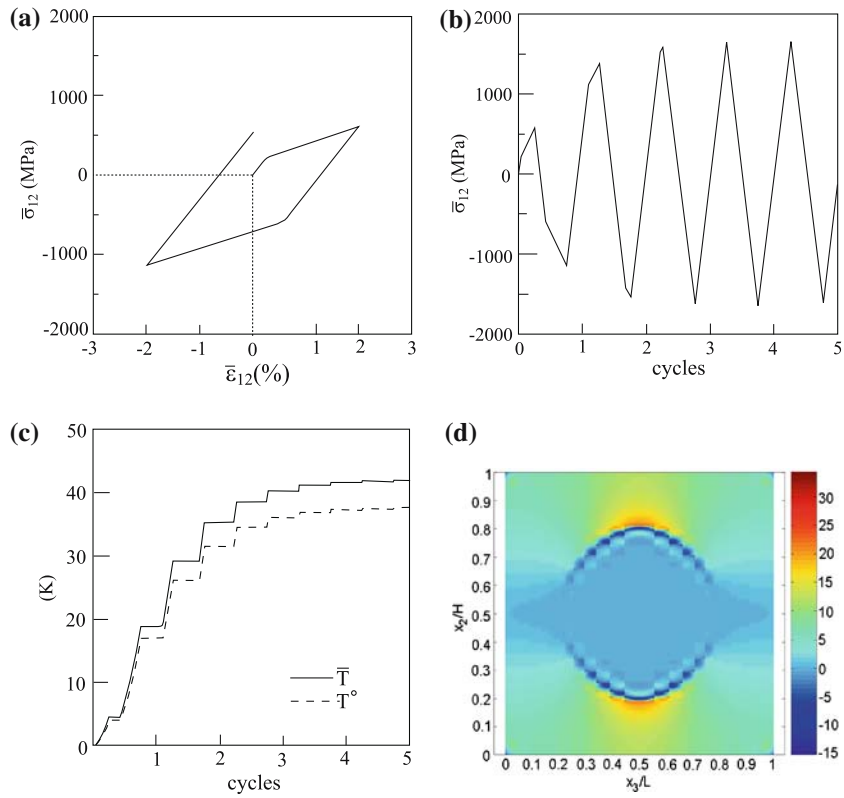

Fig. 6 The axial shear stress–strain response in: (**a**) one cycle and, (**b**) five cycles of the Al_2O_3/ aluminum composite. (**c**) The average temperature deviations $\bar{T}$ and T^0 as predicted by the two-way TMC, Eq. (105), and the homogenized energy equation (91), respectively, which are induced by an axial shear loading of the composite to a strain of $\bar{\epsilon}_{12} = 0.02$. (**d**) Surface plot of the temperature deviation variation in the RUC at $\bar{\epsilon}_{12} = 0.02$

and their detailed interaction. In most of the thermo-elastic and thermo-inelastic micromechanical analyses, the thermomechanical coupling between the mechanical and thermal effects is one-way in the sense that the temperature affects the mechanical field, whereas the mechanical field has no effect on the temperature. In the present investigation, however, a two-way thermomechanically coupled micromechanical analysis has been established for the prediction of the response of multiphase composites whose constituents are, in general, thermo-inelastic materials. To this end, the fully coupled mechanical and energy equations of the inelastic phases have been employed. As a result, the mechanical and thermal fields affect each other and their interactions are fully accounted for. The micromechanical analysis derived here which can be referred to as the fully coupled high-fidelity generalized method of cells, provides all the effective material parameters of the multiphase composite, namely, the effective stiffness tensor, the coefficient of thermal-expansion tensor and thermal-conductivity tensor, as well as the heat capacities at constant deformation and constant stress. It also provides the global thermo-inelastic constitutive equations of the multiphase composite and the associated coupled energy equation. This micromechanical analysis is based on the homogenization technique for periodic multiphase composites that provides the governing equations (equilibrium, energy, interface and periodicity conditions) in the RUC (which describes the response of the entire periodic multiphase composite). The method of solution of the established governing equations is based on a higher-order theory according to which the RUC is divided into several subcells where the displacement vector and temperature deviation are expanded into second-order forms. These governing equations, as well as the constitutive ralations of the phases, are imposed in the average (integral) sense. Consequently, the local strain tensor and temperature deviation can be related to the externally applied strain in terms of the mechanical and thermal concentration tensors together with addtional thermal and inelastic quantaties. As result, the effective stiffness tensor of the composite

and its global thermal and inelastic stresses can be readily determined. Thus, the global (macroscopic) fully coupled thermo-inelastic constitutive equations of the multiphase material have been established.

Results are given for fiber-reinforced metal-matrix and polymeric-matrix materials where the thermomechanical coupling plays different roles due to the presence or absence of inelastic effects in the corresponding matrices. A particular emphasis has been given to the induced temperature in the composite's phases as a result of the application of various types of far-field mechanical loadings.

The incorporation of the present two-way TMC micromechanical theory with a structural analysis is a subject for a future research. The result of such a two-way thermomechanically coupled micro–macro structural analysis, will enable the investigation of the effect of the full thermomechanical coupling between the mechanical and thermal effects of the constituents on the behavior (e.g., bending and buckling) of metal-matrix and polymer-matrix composite plates and shells (for example).

In the framework of smart-composite-materials research, the effects of two-way TMC in metal and polymeric-matrix composites with shape-memory alloy fibers were investigated by Aboudi and Freed [24]. The additional effect in such composites caused by the transformation-induced plasticity in the shape-memory alloy fibers was considered by Freed and Aboudi [25].

Acknowledgements The author gratefully acknowledges the support of the Diane and Arthur Belfer chair of Mechanics and Biomechanics.

References

1. Christensen RM (1979) Mechanics of composite materials. John Wiley & Sons, New York
2. Aboudi J (1991) Mechanics of composite materials: a unified micromechanical approach. Elsevier, Amsterdam
3. Parton VZ, Kudryavtsev BA (1993) Engineering mechanics of composite structures. CRC Press, Boca Raton, FL
4. Kalamkarov AL, Kolpakov AG (1997) Analysis, design and optimization of composite structures. John Wiley & Sons, New York
5. Nemat-Nasser S, Hori M (1999) Micromechanics: overall properties of heterogeneous materials. North-Holland, Amsterdam
6. Aboudi J (1996) Micromechanical analysis of composites by the method of cells–update. Appl Mech Rev 49:S83–S91
7. Arnold SM, Pindera M-J, Wilt TE (1996) Influence of fiber architecture on the inelastic response of metal matrix composites. Int J Plasticity 12:507–545
8. Aboudi J, Pindera M-J, Arnold SM (2002) High-fidelity generalized method of cells for inelastic periodic multiphase materials. NASA TM-2002-211469
9. Aboudi J, Pindera M-J, Arnold SM (2003) Higher-order theory for periodic multiphase materials with inelastic phases. Int J Plasticity 19:805–847
10. Bednarcyk BA, Arnold SM, Aboudi J, Pindera M-J (2004) Local field effects in titanium matrix composites subjected to fiber-matrix debonding. Int J Plasticity 20:1707–1737
11. Aboudi J (2005) Micromechanically established constitutive equations for multiphase materials with viscoelastic-viscoplastic phases. Mech Time-Dependent Mater 9:121–145
12. Aboudi J (2001) Micromechanical analysis of fully coupled electro-magneto-thermo-elastic multiphase composites. Smart Mater Struct 10:867–877
13. Aboudi J (2004) The generalized method of cells and high-fidelity generalized method of cells micromechanical models—a review. Mech Adv Materl Struct 11:329–366
14. Bednarcyk BA, Arnold SM (2002) MAC/GMC 4.0 User's Manual. NASA/TM-2002-212077, 2002
15. Williams TO, Aboudi J (1999) A fully coupled thermomechanical micromechanics model. J Thermal Stresses 22:841–873
16. Ene HI (1983) On linear thermoelasticity of composite materials. Int J Eng Sci 21:443–448
17. Levin VM (1967) On the coefficients of thermal expansion of heterogeneous materials. Mech Solids 2:58–61
18. Haj-Ali RM, Pecknold DA (1996) Hierarchial material models with microstructure for nonlinear analysis of progressive damage in laminated composite structures. Civil Engineering Studies, University of Illinois at Urbana-Champaign, UILU-ENG-96-2007
19. Aboudi J, Pindera M-J, Arnold SM (2001) Linear thermoelastic higher-order theory for periodic multiphase materials. J Appl Mech 68:697–707
20. Hunter SC (1983) Mechanics of continuous media, 2nd edn. Ellis Horwood Ltd, Chichester
21. Allen DH (1991) Thermo-mechanical coupling in inelastic solids. Appl Mech Rev 44:361–373
22. Gilat R, Aboudi J (1996) Thermomechanical coupling effects on the dynamic inelastic response and buckling of metal matrix composite infinitely wide plates. Compos Struct 35:49–63
23. Mitchell AR, Griffiths DF (1980) The finite difference method in partial differential equations. John Wiley, Chichester

24. Aboudi J, Freed Y (2006) Two-way thermomechanically coupled micromechanical analysis of shape memory alloy composites. J Mech Mater Struct 1:937–955
25. Freed Y, Aboudi J (2007) Thermomechanically coupled micromechanical analysis of shape memory alloy composites undergoing transformation induced plasticity. Submitted